Natural Resources Canada | Ressources naturelles Canada

GEOLOGICAL SURVEY OF CANADA
OPEN FILE 8914

Rare earth element (REE) content of shale, coal and coal byproducts, and potential for Canadian REE supply – a literature review and initial assessment

O.H. Ardakani, K. Biggart, and K.E. Dewing

2022

Canada

ISSN 2816-7155
ISBN 978-0-660-44935-7
Catalogue No. M183-2/8914E-PDF

GEOLOGICAL SURVEY OF CANADA
OPEN FILE 8914

Rare earth element (REE) content of shale, coal and coal byproducts, and potential for Canadian REE supply – a literature review and initial assessment

O.H. Ardakani, K. Biggart, and K.E. Dewing

2022

Permanent link: https://doi.org/10.4095/330549

This publication is available for free download through GEOSCAN (https://geoscan.nrcan.gc.ca/).

Recommended citation
Ardakani, O.H., Biggart, K., and Dewing, K.E., 2022. Rare earth element (REE) content of shale, coal and coal byproducts, and potential for Canadian REE supply – a literature review and initial assessment; Geological Survey of Canada, Open File 8914, 61 p. https://doi.org/10.4095/330549

Publications in this series have not been edited; they are released as submitted by the author.

Table of contents

1. Introduction

Rare earth elements (REE, or REY if including Yttrium) are comprised of the lanthanide series of elements on the periodic table (La, Ce, Pr, Nd, Pm, Sm, Eu, Gd, Tb, Dy, Ho, Er, Tm, Yb, and Lu), as defined by the International Union of Pure and Applied Chemistry (IUPAC). Scandium and Y, although not lanthanides, are commonly considered to be REE as well due to their similar chemical properties (Balaram, 2019). The REE are often referred to as a single group (Fig. 1), but in practice, each individual element has a specific set of end-uses (Fig. 2), and so the global demand varies between them.

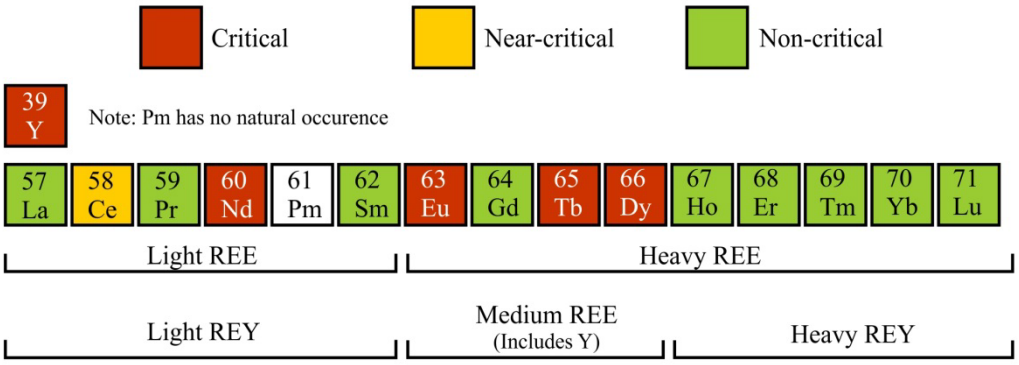

Figure 1. *Classification of lanthanides and yttrium in light, medium, and heavy REY, and light and heavy REE groups with their importance (after Seredin and Dai, 2012).*

1.1 The importance of rare earth elements (REE)

The REE have an essential role in permanent magnets, rechargeable NiMH batteries, lamp phosphors, as well as 'smart' electronic devices and defense industries (Fig. 2). REE are needed for automotive catalysts or fluorescent lamps that are used in hybrid cars and wind turbines (U.S. Department of Energy, 2011; Binnemas et al., 2013; Dutta et al., 2016, *NRCan REE facts*). However, the major demand for REE is likely linked to the use of NdFeB magnets, which is particularly used in hybrid and electric vehicles, wind turbines, and in erbium-doped glass fiber for communications (Goodenough et al., 2018). The REE have attracted much attention in recent years, being viewed as critical metals because of China's domination of the supply chain (Goodenough et al., 2018).

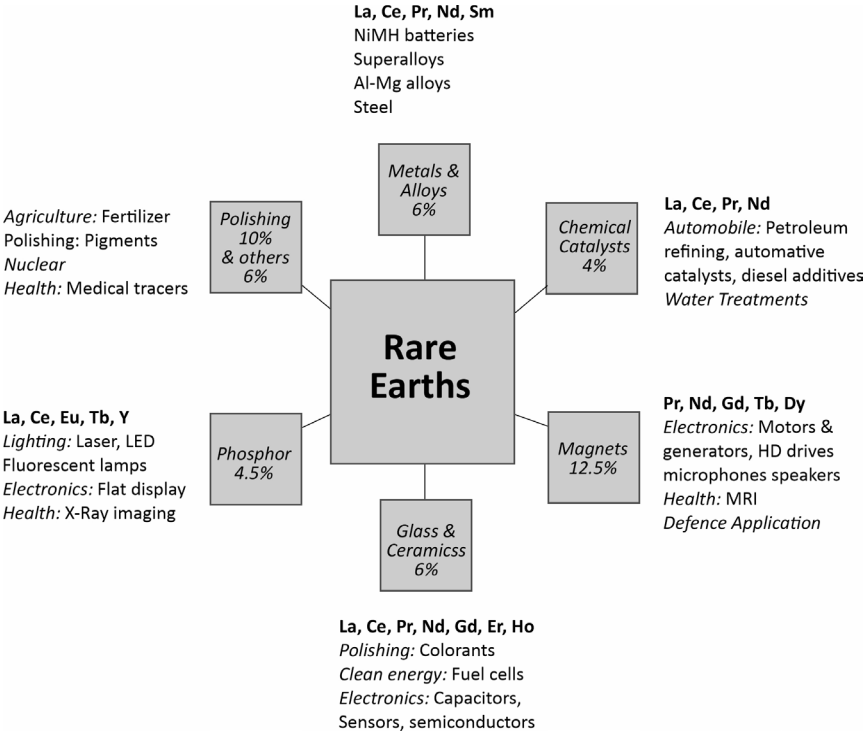

Figure 2. *Major industrial uses of REE. The percentage value in each sector is the forecasted industry-level annual growth rate (modified after Dutta et al., 2016).*

The European commission (2014) and the U.S. Department of Energy (U.S. Department of Energy, 2011, 2011) considers REE as the most critical raw materials (CRM) group, with highest supply risk. In the U.S. Department of Energy medium-term critically matrix (Fig. 3), the five most critical REE are neodymium (Nd), europium (Eu), terbium (Tb), dysprosium (Dy), and yttrium (Y) (U.S. Department of Energy, 2011).

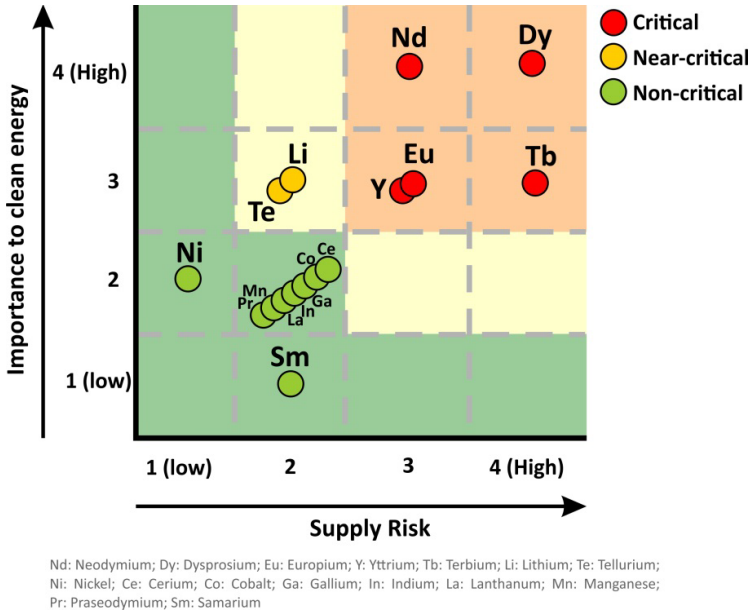

Figure 3. *U.S. Department of Energy medium term (2015–2025) criticality matrix, showing the five most critical rare-earth elements (Y, Nd, Eu, Tb, Dy), (modified after U.S. Department of Energy, 2011).*

Due to the critical role REE play in transition to low carbon energy and high technology industries, the global REE demand is growing at an approximate annual rate of 5% by 2020 (Dutta et al., 2016). With global population growth, new consumption habits, technological change and economic development in some parts if the world, the demand for CRM significantly increased. The concern about resource security has recently regained importance.

China presently has the highest reserves (Table 1) of REE and supplies more than 58% of the global REE demand (U.S. Department of Energy, 2017, *NRCan REE facts*). With a single global REE provider with the highest global reserves, the world is confronted with a REE supply risk. Therefore, other countries are now actively seeking new exploitable REE deposits and also alternative sources of REE (Seredin and Dai, 2012; Emsbo et al., 2015; Dai et al., 2016a, b; Hower et al., 2016, 2020a, b) and also REE recycling from end of life products (Binnemans et al., 2013; Folgueras et al., 2017).

Table 1. *Major REE producers, their production, and total reserve by country (USGS, 2022).*

Country	Mine Production 2020	Mine Production 2021	Reserves (Tonnes)	% of Total Reserves
China	140,000	168,000	44,000,000	35.20%
Vietnam	700	400	22,000,000	17.60%
Brazil	600	500	21,000,000	16.80%

Russia	2,700	2,700	21,000,000	16.80%
India	2,900	2,900	6,900,000	5.52%
Australia	21,000	22,000	4,000,000	3.20%
United States	39,000	43,000	1,800,000	1.44%
Greenland	-	-	1,500,000	1.20%
Tanzania	-	-	890,000	0.71%
Canada	-	-	830,000	0.66%
South Africa	-	-	790,000	0.63%
Other Countries	100	300	280,000	0.22%
Burma	31,000	26,000	N/A	N/A
Madagascar	2,800	3,200	N/A	N/A
Thailand	3,600	8,000	N/A	N/A
Burundi	500	100	N/A	N/A
World Total	**244,900**	**277,100**	**124,990,000**	**100%**

1.2 Primary REE resources and the potential secondary (alternative) REE resources

REE deposits can be classified as primary and secondary REE exploration targets (Simandl, 2014 and references therein). In this classification, primary REE exploration targets are those deposits in which REE are the principal elements of economic interest, whereas secondary REE exploration targets are those that REE are possible co-product commodities (Simandl, 2014). The primary REE resources include those formed by high-temperature geological processes (carbonatites, alkaline rocks, vein and skarn deposits) and those formed by low-temperature processes (placers, laterites, bauxites and ion-adsorption clays) (Simandl, 2014; Goodenogh et al., 2018). The majority of the REE global supply is still derived from primary resources (Goodenough et al., 2018); however there is a substantial research focus on recycling of REE from end-life product resources (e.g., Binnemans et al. 2013) and also mine waste (Folgueras et al., 2017).

Coal deposits have attracted much attention in recent years as promising alternative sources for REE and Y (Seredin and Dai, 2012; Dai et al., 2016a, b, c; Hower et al., 2016; Dai and Finkelman, 2017). Coal is a resource primarily used for electric power generation, and currently supplies 41% of global electricity needs. In addition, significant quantities of coal are still being used metallurgical processes, cement industries, and as raw material for activated carbon (Dai and Fikelman, 2017 among many others). Coal can also be considered as an economic source of

strategically important elements, such as REE, Ge, Ga, Y, Sc, Nb, Re (Dai et al., 2016a, b, c; Hower et al., 2016, 2020a, b; Dai and Finkelman, 2017).

1.3 Canada primary REE resources and production

Canada has abundant reserves of REE and Nb and there are currently several exploration projects underway across the country (Fig. 4) (Zinck, 2013; NRCan, 2022). However, the only active primary REE production in Canada at present is at the Niobec Mine in the Saguenay region of Quebec. Other identified REE primary resources in Canada are in the stage of exploration and the prediction that some would be operational by 2020 has not borne out (Zinck, 2013; Canadian Rare Earth Element Network). The Canadian Rare Earth Element Network (CREEN) aims to produce and secure 20% of the global supply market for separated critical REE products in the near future. In order to reach this level in global REE production, Canada needs to search for other potential REE and Nb resources.

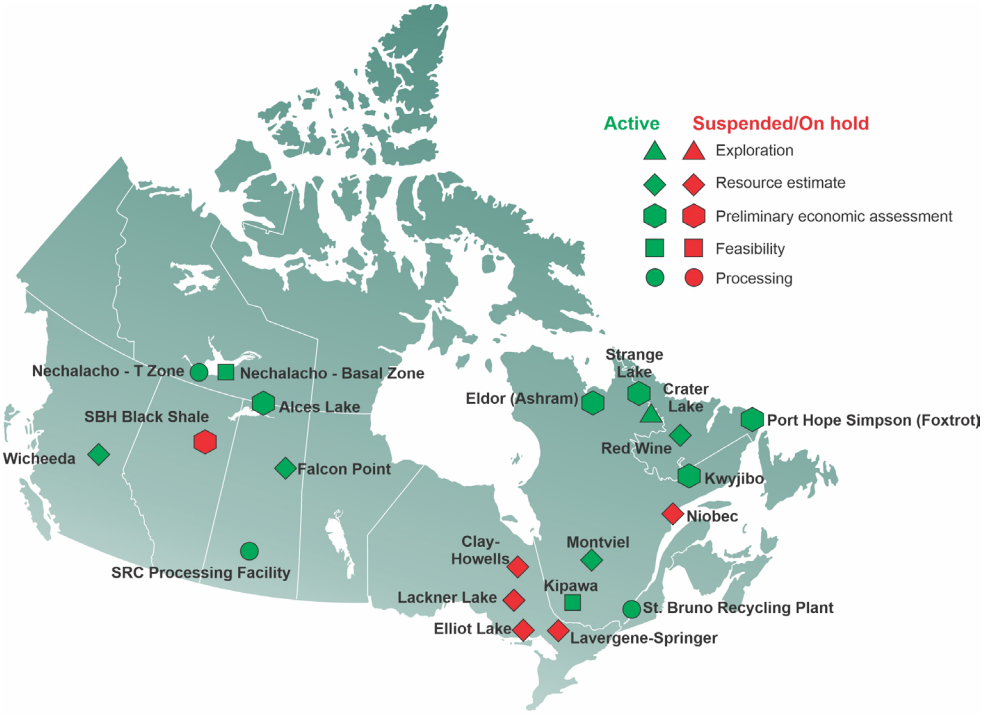

Figure 4. *Selected advanced Canadian rare earth projects (after NRCan REE facts, 2022).*

1.4 Major Global Studies on REE Secondary Resources

Seredin and Dai (2012) classified REY into three groups: light rare earth elements (LREE - La, Ce, Pr, Nd, and Sm), medium rare earth elements (MREE - Eu, Gd, Tb, Dy, and Y), and heavy rare earth elements (HREE - Ho, Er, Tm, Yb, and Lu). In the literature, HREE is commonly considered as a combination of MREE and HREE elements (Eu to Lu), and LREE concentrations are compared to HREE concentrations to determine relative enrichment of the two groups (Fig. 1).

Because HREE are economically more significant than LREE, the relative enrichment of HREE to LREE is an important factor to consider when evaluating REY concentrations in REY-rich deposits. Seredin (2010) proposed a classification of REY elements into critical (Nd, Eu, Tb, Dy, Y and Er), uncritical (La, Pr, Sm, and Gd) and excessive (Ce, Ho, Tm, Yb, and Lu), based on industry's demand for the particular element.

The promising REY deposits should have a predominance of critical REY elements (Mastalerz et al., 2020; Seredin and Dai, 2012), which can also be used to economically grade a deposit by evaluating the relative ratio of critical elements to excess elements, known as the outlook coefficient (Seredin, 2010). Conversely, a REY-rich deposit should have as few as possible of the excess REY, especially Ce, the most abundant REE in nature (Seredin and Dai, 2012).

The REY have historically been utilized in studies as geochemical indicators of provenance, paleo environment and post-depositional history of the sedimentary environment (e.g., in shales and coals) (McLennan, 1989; Lev and Filer, 2004; Bau et al., 2014; Wang et al., 2014; Noack et al., 2015; Dai et al., 2016a,b,c; Phan et al., 2019). REY typically exhibit coherent behavior and are relatively immobile during different geochemical processes (Lev and Filer, 2004; Dai et al., 2016), display uniform composition in shales similar to that of the upper crust (Taylor and McLennan, 1985), and have predictable patterns of fractionation, which make them exemplary geochemical indicators (Dai et al., 2016a,b,c). Geochemical studies of water have also used REY as tracers due to their predictable fractionation and cycling in the marine, submarine groundwater and sediment pore water systems (Piper, 1974; Freslon et al., 2014; Yang et al. 2017; Caetano-Filho, 2018).

In addition to their uses as geochemical indicators, REY themselves are valuable elements. Demand in REY has been significantly growing over the past few decades due to their unique magnetic, catalytic and phosphorescent properties (Balaram, 2019). They are a valuable and critical economic resource utilized in a variety of technological goods, such as electronics, LED

light bulbs, wind turbines, hybrid cars, rechargeable batteries, etc. (Birdwell 2012; Balaram, 2019; Costis et al., 2019). Baron (2020) provides an example list of individual REY industrial uses.

China currently dominates global REY production, producing and exporting over 90% of the world's REY consumption (Costis et al., 2019; Hussain and Luo, 2020). REY are produced mainly from two ore deposits in China: an carbonatite deposit with abundant LREE and a clay-type deposit rich in HREE (Emsbo et al., 2015 and references therein). Due to increasing global demand for REY and Chinese restrictions on REY exports, other countries have been taking initiatives in exploring for and producing REYs from their own reserves.

1.5 Current Study

This study is part of Targeted Geoscience Initiative (TGI) program under the volcanic and sedimentary ore systems and their critical minerals activity to investigate critical raw element (CRE) resource assessment of major Canadian coal and organic-rich shales. Although the research on sedimentary CRE resource potential started in other countries with abundant coal and shale deposits since 2015, few studies to-date has been done on the equivalent Canadian resource potential (Flier-Keller, 1993) while the majority of recent studies was local in nature (Birk and White, 1991; Kuppusamy and Holuszkon, 2019a,b, 2020, 2021, 2022) rather than a comprehensive national study.

This study with comprehensive literature review will address key knowledge gaps concerning sedimentary CRE resources to support the strategic and sustainable development of CRE in Canada. The main objectives are: (1) evaluate the CRE content of those resources; and (2) choose the most promising resources for CRE extraction in collaboration with federal government research institutes, industry and provincial jurisdictions. The first part of this report presented the major studies on coal and coal combustion REE resources, their origin, mode of occurrence and economic evaluation of those resources. In the second part of the report, REE contents from Geological Survey of Canada datasets of Canadian Phanerozoic organic-rich shales and siliciclastic rocks are presented in order to identify most promising REE sedimentary sources. The siliciclastic sedimentary units and most promising intervals will be examined for resource evaluation and identification of origin, mode of occurrence and development of best extraction methodologies to expand the REE production of potential Canadian resources.

2. Relative REY Enrichment in Different Types of Rock Units

Traditionally, REY are mined from carbonatite and alkaline igneous deposits that host REY-bearing accessory minerals such as bastnäsite, xenotime, monazite and others (Dostal 2017; Sarswat et al., 2020). In the USA, traditional REY production is limited to the Mountain Pass mine in California, in which REY are produced from bastnäsite ore (Lefticariu et al., 2020). Although the mine is prolific in REY, it has had an unstable history of production due to environmental regulations and company bankruptcies; it has also lost its processing capacity to China.

Other REE-rich minerals include clays (e.g., kaolinite, illite, etc.), resistates (e.g., florencite, zircon, etc.), water-bearing phosphates (e.g., rabdophane), carbonates (Dai and Finkelman, 2017; Goodarzi and Gentzis, 2018; Seredin and Dai, 2012; Yang et al., 2018). Coal and organic-rich shales (also known as oil shales or black shales in the literature) have recently been targeted as potential REY sources (Fu et al., 2010; Bai et al., 2011; Birdwell, 2012; Yang et al., 2018; Berna 2019). Secondary sources that have been evaluated for potential REY extraction include byproducts from the mining industry, such as coal fly ash, acid mine drainage, coal combustion products, bauxite residue, uranium mine processing streams and tailings, phosphor-gypsum, and heavy mineral concentrate byproducts (e.g., Goodarzi, 2002; Cameron, 2017; Dai and Finkelman, 2017; Mutlu et al., 2018; Costis et al., 2019; Yang et al., 2018; Lefticariu et al., 2020; Li et al., 2020; Middleton et al., 2020; Park et al., 2020; Rosita et al., 2020; Sarswat et al., 2020). Yang et al. (2018) even evaluated whether or not hydraulic fracturing fluids could release REE as byproducts from shales (with results suggesting insignificant REE release).

2.1 REY in Coal Deposits

In the USA, more than 45,000 tons of REE hosted in coal were mined in 2018, with an average concentration of 62 ppm (Roth and Alvin, 2020). Some coal basins contain high REY contents (> 0.1 wt.%) in coal seams, coal ash, and host and basement rocks (Seredin and Dai, 2012). As the largest source of REY following traditional igneous deposits, coal has extensively been studied in the literature (mainly conducted in China), with studies focusing on REY concentration, distribution, modes of occurrence, mineral and organic hosts, relative enrichment, origin, genetic influences and modes of enrichment, anomalies of particular elements, comparisons to coals worldwide, and REE extraction and recovery (e.g., Baron, 2020; Dai et al., 2012a,b; Dai et al.,

2016a,b,c; Finkelman et al., 2019; Hower et al., 2016; Hussain and Luo, 2020; Goodarzi and Gentzis, 2018; Mastalerz et al., 2020; Mishra et al., 2019; Roth and Alvin, 2020; Seredin and Dai, 2012; Yang et al., 2018; Zhang and Honaker, 2019).

2.1.1 REY Enrichment and Modes of Occurrence in Coals

Seredin and Dai (2012) concluded that four main genetic modes of REY enrichment occur in coal: 1) terrigenous, associated with detrital minerals and REY input by surface waters; 2) tuffaceous, associated with leaching of volcanic ash; 3) infiltration, associated with meteoric water; and 4) deep hydrothermal fluids. Fine-grained authigenic minerals are the primary REY-hosts, including clays, aluminum phosphates and water-bearing phosphates (e.g., rhabdophanes and cherchite), aluminum sulphates, water-bearing carbonates, zircon, apatite and fluorocarbonates (Seredin and Dai, 2012; Hower et al., 2016; Hower et al., 2020a). Heavier REY tend to be preferentially desorbed from clays by acidic waters (Hower et al., 2016). REY in many prolific coals can also be associated with organic matter (Hower et al., 2020a; Seredin and Dai, 2012a).

HREE are more closely associated with organic matter and occur in more easily dissolvable forms than are LREE; therefore peats and low-rank coals (i.e., low thermal maturity) are more likely enriched in HREE relative to LREE (Zhang and Honaker, 2019; Hower et al., 2020a and references therein;). In contrast, Dai et al. (2008) reported a greater affinity of LREE rather than HREE for organic matter in coals from China. Although coals can present with high concentrations of REY, this is most commonly limited to thin partings and coal benches near the floor or base of thick coal seams, or directly beneath and associated with volcanic tonsteins (Seredin and Dai, 2012; Hower et al., 2016). Since REY composition and concentration can vary significantly vertically and laterally within a coal seam (Dai et al., 2012b), it is necessary to sample thin benches for selective REY-rich prospecting within coal sequences (Seredin and Dai, 2012).

2.1.2 Normalized REY Distribution Patterns

For comparative purposes, REY concentrations and distribution patterns within coals are compared to world standards, including different coals worldwide and the upper continental crust (UCC) (Table 1). The average sum of REY (∑REY) in world coals was determined to be 68.5 ppm

by Ketris and Yudovich (2009), whereas rocks of the UCC present an average ∑REY of 168.4 ppm (Taylor and McLennan, 1985). The average ∑REY of USA coals is 62.1 ppm (Finkelman, 1993) similar to the global average, whereas the average ∑REY of Chinese coals is significantly higher at 137.9 ppm (Dai et al., 2008).

Average concentrations of REY in coal ash, on the other hand, are significantly enriched in comparison to the raw coals and the UCC; for instance, the average ∑REY of world coal fly ash is 404 ppm and USA coal fly ash 517 ppm (Seredin and Dai, 2012). Seredin and Dai (2012) attributed this enrichment to either an abnormal REY-enrichment of the coals themselves, or to coals with low ash yields.

In comparison to the UCC, coals and coal ash can be enriched or depleted with respect to LREE, MREE and HREE. Seredin and Dai (2012) classified REY enrichment based on REY distribution patterns: LREE enrichment (L-type distribution; $La_N/Lu_N > 1$), which is most typical for REY-rich Chinese coal ashes; MREE enrichment (M-type distribution; $La_N/Sm_N < 1$, $Gd_N/Lu_N > 1$), in which the origin of the M-type distribution of high-REY rocks is likely due to acid hydrothermal influences; and HREE enrichment (H-type distribution; $La_N/Lu_N < 1$), which is also typical of coal ashes and may be attributed to a variety of HREY-enriched natural waters circulating throughout coal basins (Seredin and Dai, 2012).

A normal (N-type) distribution pattern in which there is only weak or no fractionation between the different REY-types can also be identified, but is rarely observed for REY-rich coals (Dai et al., 2016a). Although the origin of the distribution type of the coals can be surmised, coals and their corresponding ashes present as the most complicated relative to all rocks and exhibit a significant variability in distribution type (Seredin and Dai, 2012). Thus, caution must be exercised in determining REY-distribution origin, and distribution patterns should only be compared to conventional REY ores (Seredin and Dai, 2012).

Table 2. *Average REY concentrations of normalization standards (UCC, NASC) and common coals.*

Deposit Type	Average ∑REE Concentration	Reference
Upper Continental Crust (UCC)	168.4 ppm	Taylor and McLennon, 1985
North American Shale Composite (NASC)	165.4 ppm	Gromet et al., 1984
World Coal	68.5 ppm	Ketris and Yudovich, 2009

Chinese Coal	137.9 ppm	Dai et al., 2008
USA Coal	62.1 ppm	Finkelman, 1993
World Coal Ashes	404 ppm	Seredin and Dai, 2012
Chinese Coal Ashes	517 ppm	Seredin and Dai, 2012
Worldwide Black Shale	134.19 ppm	Ketris and Yudovich, 2009

Individual REY concentrations can be normalized to those of the UCC and other normalization standards such as chondrite, PAAS (Post Archean Australian Shale) and NASC (North American Shale Composite) as presented in Table 2 (Taylor and McLennon 1985). Note that Boynton (1985) provided alternative (although similar) values as Taylor and McLennon (1985) for chondrite, and Gromet et al. (1984) for NASC (not presented herein). Corresponding distribution patterns (plots of REY versus their normalized concentrations) can then be compared (Dai et al., 2016a; Mastalerz et al., 2020; Mishra et al., 2019; Roth and Alvin, 2020; Seredin and Dai, 2012).

In Figure 5, REY distribution patterns of world coals, Chinese coals, and USA coals normalized to UCC presented by Dai et al. (2016a). Another normalization standard that has been used for coals in the literature is the Post Archean Australian Shale (PAAS; Taylor and McLennon, 1985; e.g., used by Goodarzi and Gentzis (2018) in their studies of Canadian Arctic coals and oil shales). Both UCC and PAAS REY values and distribution patterns present similar results and are therefore both appropriate to use as normalization standards for coals.

However, as noted by Dai et al. (2016a, p. 84), "coal was deposited within the upper continental crust and contains many detrital UCC contributions mixed within the peat environment"; therefore, it is recommended that REY distribution patterns of coal and its associated material (e.g., fly ash) be normalized to the UCC for global comparative purposes.

Although normalization to chondrite has also been utilized (e.g., Goodarzi et al., 1990), Dai et al. (2016a) recommended against this as the normalization standard should be chosen based on a similar genetic origin to the coal samples being normalized, which chondrites are not. The quality of REY data can be simply evaluated by observing the smoothness of the normalized REY distribution pattern (Dai et al., 2016a; Roth and Alvin, 2020). For instance, distribution curves that exhibit large deviations from a smoothed curve or have a sawtooth pattern (Fig. 6) likely indicate

analytical error in the data collection and should therefore be assessed with caution (Roth and Alvin, 2020).

Table 3. *Average REY concentrations (ppm) of the following normalization standards: chondrite, UCC (Upper Continental Crust), PAAS (Post Archean Australian Shale) and NASC (North American Shale Composite). All values are from Taylor and McLennon (1985).*

Standard	Y	La	Ce	Pr	Nd	Sm	Eu	Gd	Tb	Dy	Ho	Er	Tm	Yb	Lu
Chondrite	2.1	0.367	0.957	0.137	0.711	0.231	0.087	0.306	0.058	0.381	0.085	0.249	0.036	0.248	0.038
UCC	22	30	64	7.1	26	4.5	0.88	3.8	0.64	3.5	0.8	2.30	0.33	2.2	0.32
PAAS	27	38	80	8.9	32.0	5.6	1.1	4.7	0.8	4.4	1.0	2.9	0.4	2.8	0.4
NASC	-	33.04	70.55	8.70	31.76	5.99	1.38	5.50	0.94	5.54	1.16	3.52	0.53	3.15	0.49

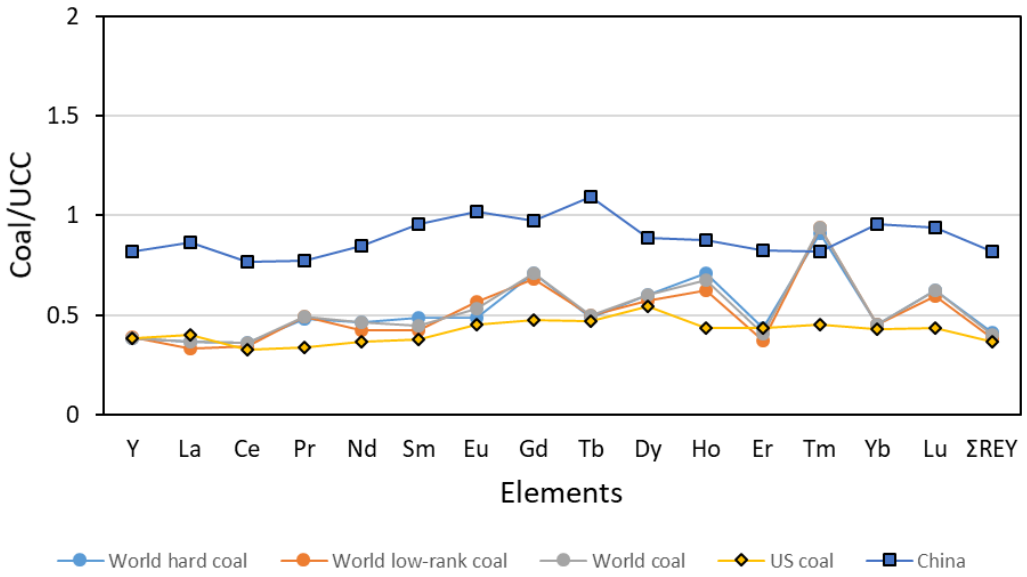

Figure 5. *REY distribution patterns of world coals, Chinese coals and USA coals normalized to the UCC (data for plot from Dai et al., 2016a).*

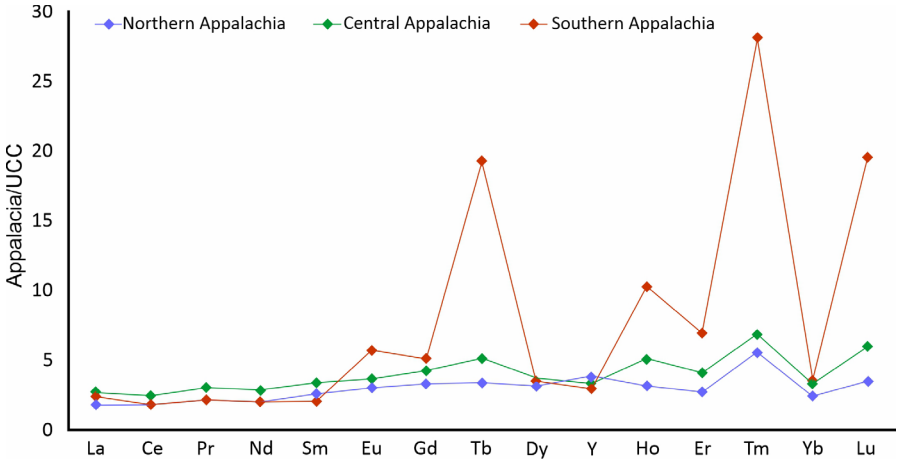

Figure 6. *Example REY distribution curves (normalized to UCC), showing a suspect sawtooth distribution curve for the Southern Appalachia samples (from Roth and Alvin, 2020).*

2.1.3 REY Anomalies

REY anomalies in comparison to standard values (positive or negative) can also be used alongside normalized REY-distribution patterns for comparative purposes, as well as for making inferences on depositional environment and sediment source region, geochemical history and tectonic evolution of the coal deposits (Dai et al., 2016a and references therein; Mastalerz et al., 2020). Since the distribution patterns of REY have a predictable pattern of fractionation, only certain types of anomalies are expected (Dai et al., 2016a). Anomalies of the redox-sensitive elements Eu and Ce are common; anomalies of non-redox-sensitive elements can also occur, namely for La, Y and Gd (Hussain and Luo, 2020).

Of the REY elements, Ce is the only element that can be oxidized to the tetravalent state (Ce^{4+}) under certain conditions (low temperature, highly-oxidizing, alkaline PH conditions in shallow crustal environments) (Dai et al., 2016a and references therein). Cerium-enriched sedimentary deposits can be inferred to have formed in oxic environments, whereas those formed in reducing or anoxic environments display Ce-depletion (Birdwell, 2012).

Cerium anomalies are denoted by Ce_N/Ce_N^*, where N refers to the normalization standard used (ex. UCC, PAAS, etc.); Ce_N is the normalized value of Ce in the investigated samples; and Ce_N^* is the Ce concentration of the normalization standard (Dai et al., 2016a). Dai et al. (2016a) provide calculations of the Ce anomaly in equations 1 and 2:

$$Ce_N/Ce_N^* = Ce_N / (0.5La_N + 0.5Pr_N) \quad \text{(Equation 1)}$$

The Ce anomaly can alternatively be calculated with equation 2 if Pr data is not available:

$$Ce_N/Ce_N^* = Ce_N / (0.67La_N + 0.33Nd_N) \quad \text{(Equation 2)}$$

The normalized Cerium in coal often exhibits weakly negative or negative anomalies; positive Ce anomalies in coal are rare (Dai et al., 2016a). The dominant control on Ce anomalies is the sediment sources, where negative anomalies are commonly associated with coals formed in an environment influenced by marine incursion (Dai et al., 2016a; Mishra et al., 2019).

Coals with weak negative Ce anomalies can be inferred to be from sediment source regions dominated by felsic material (Dai et al., 2016a). Input of terrigenous basaltic material, however, does not result in distinct Ce anomalies, as the original material is not Ce-anomalous (Dai et al., 2016a). Thus, the Ce anomaly in coals can be used to infer the general composition of the sediment sources. Other factors can affect Ce anomalies and should be considered, such as: weathering and oxidation of Ce^{3+} to Ce^{4+}, Fe–Mn oxyhydroxide mineralization and the influence of water (Dai et al., 2016a; Mishra et al., 2019).

Whereas deep hydrothermal fluids do not exhibit negative Ce anomalies and therefore do not produce Ce anomalies in hydrothermal-altered coal, coal strata affected by surface waters may display negative to strongly negative Ce anomalies (Dai et al., 2016a). Europium anomalies are denoted by Eu_N/Eu_N^*, where N is the normalization standard used; Eu_N is the normalized value of Eu in the investigated samples; and Eu_N^* is the Eu concentration of the normalization standard (Dai et al., 2016a). Dai et al. (2016a) provide a calculation of the Eu anomaly in equation 3:

$$Eu_N/Eu_N^* = Eu_N / (0.5Sm_N + 0.5Gd_N) \quad \text{(Equation 3)}$$

The Eu anomaly can alternatively be calculated with equation 4, in order to prevent a Gd anomaly interfering with the Eu anomaly (Dai et al., 2016a and references therein):

$$Eu_N/Eu_N^* = Eu_N / [(Sm_N \times 0.67) + (Tb_N \times 0.33)] \quad \text{(Equation 4)}$$

Anomalous Eu concentrations are generally associated with the sedimentary sources. As is the case for the other lanthanides, Eu exists in the trivalent state (Eu^{3+}) (Birdwell, 2012). Unlike the other REY, Eu can be reduced from Eu^{3+} to Eu^{2+} in strongly reducing conditions under low

temperatures (< 250ºC); this occurs mainly during magmatic processes and not during natural surface processes (Dai et al., 2016a).

Europium anomalies are therefore not generally associated with weathering or transport processes, but are inherited from the original source rocks (Dai et al., 2016a; Taylor and McLennon, 1985). Coals with positive Eu anomalies are interpreted to have formed within sediment source regions dominated by mafic basaltic terrigenous rock, whereas negative Eu anomalies formed with input from felsic terrigenous rock (Dai et al., 2016a). In their investigations of coals from the Tahir Coal Basin in India, Mishra et al. (2019) attributed negative Eu anomalies to a felsic source region that was depleted in Eu due to partial melting, fractional crystallization of feldspar, or Eu mobility during coal formation.

Distinct positive Eu anomalies are also commonly attributed to the injection of hydrothermal fluids (Bau et al., 2014; Hussain and Luo, 2020). Other possible causes of positive Eu anomalies within coals include the influence of volcanogenic hydrothermal solutions in the peat swamp, or sometimes a high apatite or illitic clay content (Dai et al., 2016a). Alternatively, Dai et al. (2016) cautioned that positive Eu anomalies in Ba-rich coals could be a product of analytical error during ICP-MS analysis, and in such coals a correction must be applied for mass interferences by BaO and BaOH.

Other common REY anomalies in coal include anomalous concentrations of Y, Gd and La which are not redox-sensitive elements like Ce and Eu (Dai et al., 2016a). The Y anomaly is defined by the Y_N/Ho_N ratio (in which N refers to the normalized value), where a negative anomaly is indicated by $Y_N/Ho_N < 1$ and a positive anomaly $Y_N/Ho_N > 1$ (Dai et al., 2016a). Similar to Eu and Ce, Y anomalies can be influenced by various factors, including the sediment source region, environment and influence by hydrothermal fluids.

Common Chinese and USA coals exhibit very weak Y anomalies (Dai et al., 2016a) relative to the UCC, and hydrogenetic deposits are characterized by negative Y anomalies (Bau et al., 2014). Weakly positive Y anomalies are attributed to sediment source regions with basaltic input, whereas felsic source regions generally only produce very weak or no Y anomalies (Dai et al., 2016a). Positive Y anomalies could be attributed to input by Y-bearing phosphates, or influence by seawater or hydrothermal fluids.

Coal can also exhibit Gd anomalies, which generally present as positive, weakly positive or sometimes weakly negative, or as no anomaly (Dai et al., 2016a). In Chinese and USA coals, Gd

anomalies are often negative (Dai et al., 2016a). Positive Gd anomalies are associated with hydrothermal fluids and seawater, but can also be due to analytical error resulting from Th influence (Dai et al., 2016a). Gd anomalies are represented by Gd_N/Gd_N^*, where N refers to the normalization standard used; Gd_N is the normalized value of Gd in the investigated samples; and Gd_N^* is the Gd concentration of the normalization standard (Dai et al., 2016a). Dai et al. (2016a) provide a calculation of the Gd anomaly in equation 5:

$$Gd_N/Gd_N^* = Gd_N / [(Sm_N \times 0.33) + (Tb_N \times 0.67)] \quad \text{(Equation 5)}$$

Lastly, La anomalies can also occur in coal, though this has rarely been investigated (Dai et al., 2016a; Seredin and Dai, 2012). Chinese and USA coals typically exhibit positive La anomalies, relative to the UCC (Dai et al., 2016a). Lanthanum anomalies are represented by La_N/La_N^*, where N refers to the normalization standard used; La_N is the normalized value of La in the investigated samples; and La_N^* is the La concentration of the normalization standard (Dai et al., 2016a):

$$La_N/La_N^* = La_N / (3Pr_N - 2Nd_N) \quad \text{(Equation 6)}$$

In summary, the redox-sensitive REY, Ce and Eu are often anomalous in coals, and the non-redox sensitive elements Y, Gd and La may present as anomalous. Anomalies of other REY elements are not expected, however, so their presence may indicate issues with the analytical data quality (Dai et al., 2016a).

2.1.4 Grading Coal Deposits for Estimation of Ore Quality

Elevated concentrations of REY in coals are defined by Hower et al. (2016) to be REY > 900 ppm (on the ash basis). The REY-rich deposits should have a predominance of critical REY elements, which is based on current market trends of supply and demand for particular elements (Seredin, 2010). In the past decade these critical elements have included Nd, Eu, Tb, Dy, Er and Y (Seredin and Dai, 2012; Mastalerz et al., 2020). Dai et al. (2012a) and Hower et al. (2020a) noted that since critical elements are extracted by industry from coal combustion products (i.e., fly ash, bottom ash), an evaluation of the potential recovery of critical elements should be made on an ash basis rather than on a whole-rock basis. The cut-off grade for REY in coal and REY oxides (REO, sum of La_2O_3 to Lu_2O_3 plus Y_2O_3) in coal ash is commonly 115 – 130 and 1000 ppm,

respectively (Dai and Finkelman, 2017). The percentage of critical elements ($REY_{def,rel}$) in a REY deposit can be determined by evaluating their content with respect to total REY (Seredin and Dai, 2012):

$$REY_{def,rel} = [(Nd + Eu + Tb + Dy + Er + Y) / (\sum REY)] \times 100 \quad \text{(Equation 7)}$$

Seredin (2010) proposed that a primary estimate of ore quality could be made by evaluating the relative ratio of critical elements to excess elements, known as the outlook coefficient (C_{outl}):

$$C_{outl} = (Nd + Eu + Tb + Dy + Er + Y) / \sum REY / (Ce + Ho + Tm + Yb + Lu) / \sum REY \quad \text{(Equation 8)}$$

The higher the outlook coefficient, the higher the ore quality with respect to market demand. For comparative purposes of different deposits, Seredin (2010) proposed plotting the outlook coefficient against the critical percentage. The results of different deposits clustered into groups based on how promising they are with respect to REY composition and subsequent marketability (Fig. 7A) (Seredin and Dai, 2012). REY deposits are considered to be 'promising' if $0.7 \leq C_{outl} \leq 1.9$, and 'highly promising' if $C_{outl} > 2.4$ (Dai et al., 2016a; Seredin and Dai, 2012). Therefore, a cut-off grade of $C_{outl} > 0.7$ can also be applied to REY deposits. This classification scheme has been utilized in the literature to provide an initial estimate of REY potential of various coal and fly ash deposits (e.g., Dai et al., 2017; Dai and Finkelman, 2018; Li et al., 2020; Mastalerz et al., 2020).

Another parameter that can be utilized to estimate ore quality is the amount of rare earth oxides (REO) in the deposit. The abundance of metals in ores is generally estimated from the REY oxides in the ore (equation 9; Seredin and Dai, 2012), where an REO content of >1000 ppm (0.1 wt.%) on the ash basis is considered to be the cut-off grade for coal of any rank based on REY market prices (Seredin and Dai, 2012). Seredin and Dai (2012) also proposed that the cut-off grade could be lowered to REO > 800–900 ppm for coal seams with thicknesses > 5m and containing coal benches with > 1000 ppm REO. Seredin and Dai (2012) provided a calculation for REO as follows:

$$REO = \sum(La_2O_3 \text{ to } Lu_2O_3) + Y_2O_3 \quad \text{(Equation 9)}$$

Dai et al. (2017) proposed an alternative classification of REY deposits into 'unpromising', 'promising' and 'highly promising' based on the total REY-oxide content (REO) plotted against

C_{outl} (Fig. 7B). The average concentration of REO in world coal ashes is 485 ppm (Ketris and Yudovich, 2009); Seredin and Dai (2012) recommend an REO cutoff of > 1000 ppm. Based on the relative enrichment of the elements, Dai et al. (2016a) also proposed the classification of trace elements in coal into categories defined by the concentration coefficient (the ratio of element concentrations in a sample compared to average concentrations in world coals, CC).

A CC value of < 0.5 is considered to be depleted; normal = 0.5 < CC < 2; slightly enriched = 2 < CC < 5; enriched = 5 < CC < 10; significantly enriched = 10 < CC < 100; and unusually enriched = CC > 100 (Dai et al., 2016a). A coal ash could potentially be considered economically viable if it has an REO CC > 2 (Dai et al., 2016a).

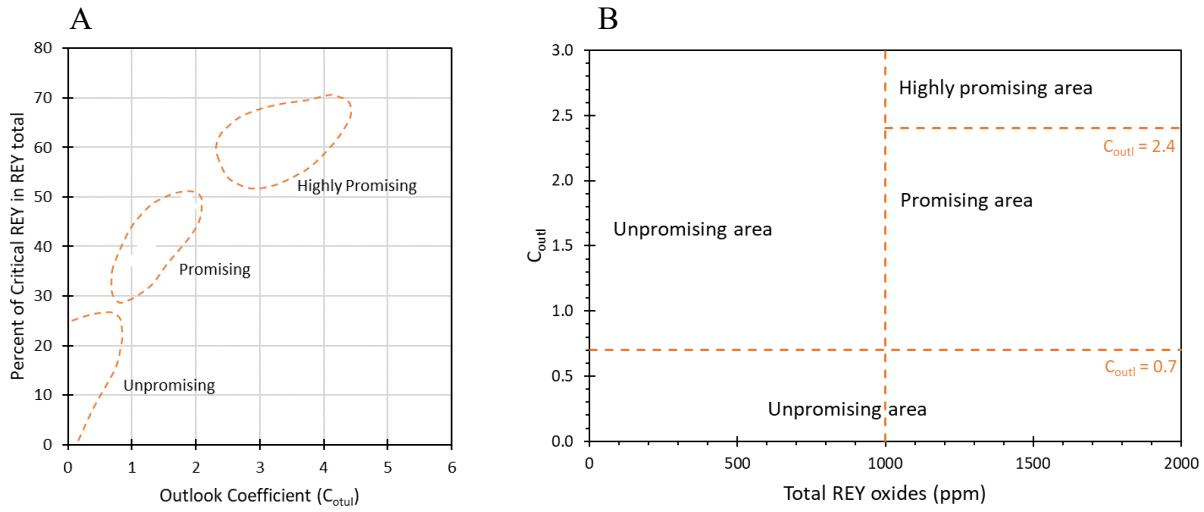

Figure 7. *Classification schemes for REY deposits (Seredin and Dai, 2012), with respect to quality in terms of economic viability. (A): Classification of REY deposits into unpromising (I), promising (II) and highly promising (III), based on the outlook coefficient (C_{outl}) and percentage of critical elements in total REY. (B) Classification of REE-rich coal ashes by Coutl vs. total REY-oxide content (after Dai et al., 2017a).*

2.1.5 Examples of REY Occurrences in Coal from the Literature

Appalachian coals in the USA are a prolific source of REY in North America (Hower et al., 2015, 2016, 2020a; Zhang and Honaker, 2019; Roth and Alvin, 2020). Average ∑REE contents of these and other coal deposits are listed in Table 3. In particular, the Fire Clay Coal and Manchester Coal zones of Kentucky are highly REY-enriched, which is attributed mainly to the presence of a volcanic ash-fall tonstein layer in the Fire Clay Coal (Hower et al., 2016; Zhang and Honaker, 2019).

REY-enriched tonsteins have also been noted by Dai et al. (2012) for associated coals in China and by Goodarzi et al. (1990) for tonsteins in Canada. In the Fire Clay Coal, some REY-rich detrital minerals (zircon and phosphate) are also present in certain localities (Hower et al., 2016). Raw coal directly above and below the tonstein-layer is highly REY-enriched, with REY concentrations ranging from 2,486 ppm to 4,108 ppm on the ash basis (Hower et al., 2016; Hower et al., 2020a).

REY concentrations of 774 ppm and 899 ppm were also reported by Hower et al. (2015) for Fire Clay fly ashes (which may have been diluted by the inclusion of other coals) at two power plants. The tonstein layer exhibits LREE-enriched (mainly Ce) monazite (with 60.8 wt.% total REO) and apatite (1 wt.% total REO). Zircon grains are also present and are HREE-enriched, with 0.33 wt.% total REO (Hower et al., 2016).

The high REY content of the associated coals is ascribed to groundwater leaching of the tonstein layer in which the leached REY became incorporated into minerals and organic matter in the coal, or volcanic REY-hosting minerals became incorporated into the peat (Crowley et al., 1989; Hower et al., 2016). Above the tonstein, lithotypes in the middle of the coal bench exhibit high LREE/HREE ratios, which potentially indicates that REY emplacement was influenced by hydrothermal processes associated with the Pine Mountain thrust sheet (Hower et al., 2020a).

The eastern Kentucky Manchester coal has a REY content (ash basis) of > 2,000 ppm, with the highest REY zones occurring towards the middle and base of the coal seam (Hower et al., 2020a). Fragments of spherical nodules extracted from the coal also present with LREE-enriched phosphate rims (Hower et al., 2020b). The authors surmised that two main REY enrichment types are present in the Manchester Coal, with the primary one characterized by Heavy and Medium Heavy type REY distribution in which significantly negative Eu, Y and Gd anomalies as well as weak or negligible negative Ce anomalies are present. The second type has a Light Medium type REY distribution with distinct negative Ce and Eu anomalies (Hower et al., 2020a).

Investigations of REY occurrences in Chinese coals and associated fly ashes were carried out by Dai et al. (2008; 2012a,b; 2016a,b; 2017), Hussain and Luo (2020) and Li et al. (2020). In general, the primary modes of REE-enrichment in Chinese coals are tuffaceous (i.e., leached intra-seam tonsteins), hydrothermal, or a mix of the two (Dai et al., 2016c). Minerals in the tuff have a greater LREE-enrichment relative to HREE, with the latter more closely associated with clay minerals (Dai et al., 2016c).

Dai et al. (2012b) determined that the mean total REY content of Chinese coals (136 ppm) is higher than that of reported values of USA and world coals, due to higher ash yields and the presence of intra-seam tonsteins in some southwestern Chinese coals. The enrichment of REY in the various coals was influenced by various factors, controlled by the source rock, marine environment, hydrothermal influence, groundwater influence and/or volcanic ash (Dai et al., 2012b). Dai et al. (2012b; p. 6-13) provide an in-depth review of the factors controlling REY enrichment of various coal deposits from several basins in China.

Examples of Chinese coals with elevated REY (and other elements including Nb (Ta), Zr (Hf) and Ga) content include Late Permian ore beds of volcanic ash origin in the lower Xuanwei Formation of Yunnan (1,216–1,358 ppm REO of La–Lu+Y), as well as coal-bearing strata in the Nanchuan coalfield of Chongqing, southwestern China (260–961 ppm REE) (Dai et al., 2012b). Dai et al. (2017) identified REY-bearing minerals in K1 and K2 coals from the Moxinpo Coalfield (Chongqing) to be mainly bastnäsite, xenotime and rhabdophane, which closely coexist with kaolinite. Most of the K1 coals exhibit M-type distribution patterns with negative Ce anomalies and positive Eu, Y and Gd anomalies, whereas the K2 coals are only weakly fractionated and display weakly negative to distinctly negative Eu anomalies, distinctly positive Gd anomalies and weak Y anomalies (Dai et al., 2017).

Of the REY elements, Y is enriched ($5 < CC < 10$) and Li, La and Yb are slightly enriched ($2 < CC < 5$). The REY enrichment origin is attributed to infiltration of hydrothermal fluids (Dai et al., 2017). Based on REO cut-off grades and C_{outl} values, the K1 and K2 coals and their floor strata are considered to be promising with respect to economic viability (but K1 roof strata and K2 partings are unpromising) (Dai et al., 2017). Li et al. (2020) observed high REY concentrations (147.2–468.6 ppm) in feed coals from power plants in southwestern China, with enrichment in fly ash and bottom ash (average of 658 ± 296 ppm). With critical REY accounting for 34–39% of the total REY and C_{outl} values of 0.89–1.11, the coal combustion products present as promising secondary sources of REY (Li et al., 2020).

Coals from the Jungar and Daqingshan Coalfields in northern China display total REY values (154–257 ppm) greater than common Chinese coals and world coals (Dai et al., 2016c). The REO values of 976–1,461 ppm and C_{outl} values of 0.77–0.93 (Dai et al., 2016b) indicate they could be economically viable REY deposits. The intra-seam partings of the Jungar coals are REE-depleted, which is ascribed to groundwater leaching during parting formation (Dai et al., 2012). The REE in

the leached fluids were then incorporated into aluminum hydrate minerals in the coal, absorbed by organic matter or precipitated from solution into REE-rich minerals (Dai et al., 2012; Dai et al., 2016c).

In their investigations of coal waste products from Jurassic and Permo-Carboniferous coals in the Ordos Basin of central China, Hussain and Luo (2020) determined that although the coals were REY-enriched with average concentrations higher than USA coal and world coal, their contents were not in a promising range. A high concentration of Ce was observed, with a relative enrichment trend of Ce > La > Pr > Gd > Sm > Sc > Nd > Dy > Eu > Tb > Tm > Yb > Er > Ho > Lu (Hussain and Luo, 2020).

Based on Dai et al.'s (2016a) enrichment classification defined by the concentration coefficient, Hussain and Luo (2020) determined that relative to world coal, REY were significantly enriched (Ho, Eu, Tb, Tm and Lu); enriched (Sm, Yb and Er); slightly enriched (Sc, Pr, Gd and Dy); and normal (Ce, Nd, Y, Co, La) for the Binxian coal (and most Hencheng REY concentrations fell in the normal range). The coals presented with negative Ce anomalies and positive Eu and Gd anomalies (normalized to PAAS), suggesting REY enrichment due to hydrothermal fluids (Hussain and Luo, 2020).

A summary by Baron (2020) of hard coal in Poland determined that coal from the Upper Silesian Industrial District has an elevated Ce content relative to the global average, and that coal from the Lublin Coal Basin has a significant concentration of La and Sc. Coal combustion products of power plants revealed a higher concentration of REY relative to hard coals, with Nd, Y and Sc providing the highest content of REY in the coal ashes (Baron, 2020). Primary REY-bearing minerals in Polish coals include kaolinite, biotite, hornblende and muscovite (Baron, 2020).

Studies by Mishra et al. (2019) of coals from the Talchir coal basin in India revealed that the average REY concentration was 91 ppm (ranging from 29.6–179.4 ppm), higher than average USA coals and world coals, but lower than Chinese coals. Total REY varied considerably with depth and was positively correlated to total ash yield but negatively correlated to sulphate, indicating a detrital REY source (Mishra et al., 2019). The coals were LREE-enriched (mainly La and Ce) in comparison to the UCC, and LREE was positively correlative with phosphorous; REY-bearing phosphates were hosted by clay minerals (Mishra et al., 2019). The coal samples displayed negative Eu anomalies and both positive and negative Ce anomalies, indicating a felsic source region and various conditions of deposition (Mishra et al., 2019).

Table 4. *Average ∑REE (or REY when Y is included) contents of various coal deposits.*

Region	Sample	∑REE Content (ppm)	Reference
USA	Fire Clay Coal	2,486 – 4,108	Hower et al., 2016
USA	Manchester Coal	> 2,000	Hower et al., 2020a
China	Lower Xuanwei Coal of Yunnan	1,216 – 1,358 (REO)	Dai et al., 2012b
China	Coals from Nanchuan Coalfield (Chongqing)	260 – 961	Dai et al., 2012b
China	Coals from Moxinpo Coalfield (Chongqing)	158 – 4,488 (REO)	Dai et al., 2017
China	Coals from Jungar and Daqingshan Coalfields	154 – 257	Dai et al., 2016c
China	Feed coals from power plants in SW China	147 – 469	Li et al., 2020
Poland	Coals from the Upper Silesian and Lublin coal basins	8 – 77	Baron, 2020
India	Coals from the Talchir coal basin	30 – 179 (REY)	Mishra et al., 2019

2.2 REY in Shale Deposits

Organic-rich shales have recently raised the interest as potential REY-deposits in China (e.g., Bai et al., 2011; Bai et al., 2018; Fu et al., 2010; Fu et al., 2011), the USA (Birdwell, 2012; Jin et al., 2017; Lev and Filer, 2004; Noack et al., 2015; Phan et al., 2019; Wang et al., 2014; Yang et al., 2017; Yang et al., 2018), Canada (Turner, 2015), Russia (Zanin et al., 2010), Turkey (Berna, 2019; Cimen et al., 2013) and Egypt (Fakhry et al., 1998). The modes of REY enrichment, occurrence and distribution in shales have been evaluated in the literature and are similar to that of coals. REY anomalies and distribution patterns in shales have also been evaluated using the same comparative analyses as coals.

2.2.1 REY Enrichment and Modes of Occurrence in Shales

The general distribution of REY in shales tends to be LREE-enriched and clay-associated (Gromet et al., 1984; Condie, 1991; Ketris and Yudovich, 2009; Bai et al., 2011; Dai et al., 2018). Through sequential chemical extraction techniques applied to the Haudian and Luozigou oil shale in China, Bai et al. (2011) and Dai et al. (2018) concluded that REY mainly occur within the inorganic mineral fraction (sulphide-, carbonate-, ferromanganese oxhydroxides- and aluminosilicate-bound fractions). REY absorbed in organic matter is negligible, however, which is contrary to findings by multiple authors (e.g., Dai et al., 2008; Seredin and Dai, 2012; Hower et al., 2020a) indicating that the organic fraction is an important REY-host in coals.

Chinese Haudian and Luozigou oil shales display a relative LREE enrichment and a moderate fractionation between LREE and HREE (Bai et al., 2011; Dai et al., 2018). The LREE are associated mainly with sulphide minerals, whereas the HREE more enriched in the carbonate, ferromanganese oxyhydroxides and aluminosilicate mineral fractions (Bai et al., 2011). Condie (1991) suggested that in cratonic shales, clays control the REY distribution in shales rather than heavy minerals (i.e., zircon, apatite, monazite), based on a positive correlation of REY with Al_2O_3 but not P_2O_5 content.

Studies of oil shales in Turkey by Cimen et al. (2013) also indicate that REY are closely associated with clay minerals, which dominantly control LREE abundance. The HREE however, are more closely associated with organic material, pyrite and apatite (Cimen et al., 2013). Birdwell (2012) concluded as well that REY are concentrated in the aluminosilicate mineral fraction and

that organic matter acts to dilute REY concentrations in shales (through studies of the Green River oil shales in the USA).

2.2.2 Normalized REY Distribution Patterns and Anomalies

Similar to coals, REY concentrations and distribution patterns within shales are compared to world standards (Table 1 and Table 2). In the literature, shales have been normalized and compared to chondrite (e.g., Bai et al., 2011; Berna, 2019; Birdwell, 2012; Fu et al., 2010; Fu et al., 2011; Ma et al., 2011; Phan et al., 2019; Taylor and McLennon, 1985; Wang et al., 2014); UCC (ex. Berna, 2019; Cimen et al., 2013; Condie, 1991; Lev and Filer, 2004; Mastalerz et al., 2020; Taylor and McLennon, 1985); PAAS (e.g., Berna, 2019; Cimen et al., 2013; Condie, 1991; Goodarzi and Gentzis, 2018; Jin et al., 2017; Noack et al., 2015; Taylor and McLennon, 1985; Yang et al., 2017; Yang et al., 2018); NASC (e.g., Bai et al., 2011; Bai et al., 2018; Berna, 2019; Birdwell, 2012; Condie, 1991; Fakhry, 1998; Fu et al., 2010; Fu et al., 2011; Gromet et al., 1984; Taylor and McLennon, 1985); 3SA (Sholkovitz, 1988); parent shale (e.g., Ma et al., 2011); and different coals worldwide.

Individual REY concentrations for the chondrite, UCC, PAAS and NASC standards (Taylor and McLennan, 1985) are presented in Table 2. The same REY enrichment types developed by Seredin and Dai (2012) for coal have been applied to shale in the literature, namely: L-type distribution ($La_N/Lu_N > 1$); M-type distribution ($La_N/Sm_N < 1$, $Gd_N/Lu_N > 1$); and H-type distribution ($La_N/Lu_N < 1$), with respect to the normalization standard (N) used. REY anomalies (namely Eu, Ce, La, Y and Gd) in shales have also been computed and applied in the literature similarly to coals, as described in section *2.1.3* and calculated using equations 1–6 presented above.

2.2.3 Examples of REY Occurrences in Shales from the Literature

Oil shale in China were mainly formed in lacustrine environments (Fu et al., 2010). Studies of the Tertiary Haudian oil shales of China by Bai et al. (2011) indicate that these shales are LREE-enriched and contain an average ∑REE value of 153.82 ppm, which is higher than the average ΣREE values in Chinese coal, USA coal and world coal (Table 5). A negative normalized Eu anomaly is attributed to the original terrigenous rock, and a weakly negative Ce anomaly is inferred to represent a reduced environment of formation not affected by lake water (Bai et al., 2011). Acid-

washing tests and sequential chemical extraction methods indicated that inorganic minerals are the primary REY-hosts in Chinese Haudian and Luozigou oil shales, with TOC playing an insignificant role in hosting REE but a more significant role in their aggregation (Bai et al., 2018).

Changshe Mountain marine oil shales from the Northern Tibet Plateau in China display average ΣREEs of 68.2 ppm (ranging from 13.1 – 118.4 ppm), which is close to that of USA coals but lower than that of worldwide black shales, the NASC and Chinese coals (Fu et al., 2010). These shales also display LREE enrichment with REY hosted mainly within fine-grained minerals (kaolinite, illite and lesser in pyrite) and organic matter (Fu et al., 2010).

Changshe Mountain shales display two distribution patterns, in which one is characterized by negligible Ce anomalies and slightly higher ΣREE, LREE/HREE and La_N/Yb_N values, and the other by weakly negative Ce anomalies and slightly lower ΣREE, LREE/HREE and La_N/Yb_N values. Both patterns display distinctly negative Eu anomalies. In comparison, samples from the Cretaceous Shengli River area display a depleted ΣREE content (46.79 – 67.90 ppm), which is lower than the NASC, worldwide black shales and Chinese coals, but comparable to world coals and USA coals (Fu et al., 2011).

The REE contents are mainly associated with clays, and only partly controlled by pyrite and organic material (Fu et al., 2011). These samples also display LREE-enrichment and significant negative Eu anomalies, suggesting a felsic origin (Fu et al., 2011). A study by Wang et al. (2014) of 22 oil shale samples across three provinces in China (Jilin, Heilongjiang and Xinjiang) indicated an average ∑REE value (171.20 ppm) similar to that of the NASC but higher than Chinese coals, with ∑LREE (153.70 ppm) and ∑HREE (117.51 ppm) contents higher than that of Chinese coals (Wang et al., 2014). In accordance with the general distribution of REE in shales, the oil shale samples are distinctly LREE-enriched (Wang et al., 2014).

The REE content of organic-rich shales has been studied for samples from the United States as well. Studies of lacustrine shales from the Eocene Green River Formation in Colorado and Utah indicate an average ∑REY concentration of 98.9 ppm, ranging from 66.3–141.3 ppm (Birdwell, 2012). Lower than what is typical of the UCC and the NASC, this depleted ∑REY content is inferred to result from dilution by organic matter and carbonates, where REY are concentrated in the aluminosilicate minerals (Birdwell, 2012).

Chondrite-normalized and NASC-normalized distribution patterns are similar to each other and accentuate the lower REY concentrations of the samples relative to the reference materials as all

samples fall below unity (Birdwell, 2012). LREE/HREE ratios are slightly higher than that of the UCC, attributed to either LREE-enrichment or depletion in HREE (Birdwell, 2012). Shales from the Appalachian Basin of the USA, however, contain significantly higher REE concentrations than the Green River shales (Table 4), such as compared to the upper Devonian Java and Huron shales (average ∑REE = 167.99 ppm; Lev and Filer, 2004); the middle Devonian Marcellus Shale (average ∑REY = 202.19 ppm; Noack et al., 2015) and combined Marcellus and West Virginia shales (average ∑REY = 227.4 ppm; Phan et al., 2019). The REE content of these Appalachian shales is comparable to or higher than that of the UCC, worldwide black shales and other North American shales, and higher than that of world coal, USA coal and Chinese coal.

Through studies of Devonian to Jurassic-aged black shales (Marcellus, Ohio, Woodford, Hushpuckney and Stark shales) in the Appalachian Basin, USA (and the Mulgrave shale from England), Yang et al. (2017) determined that whole-rock REE signatures are mainly controlled by authigenic phases, and in their absence, by siliciclastic fractions and organic material. Three main groups were identified, with the first characterized by a ∑REE content < 250 ppm (on the whole-rock basis) and MREE- and HREE-enriched patterns.

The REE are mainly hosted in siliciclastic and organic fractions in low-carbonate samples (< 4% $CaCO_3$), but were mainly hosted in carbonate phases in samples with higher carbonate content (> 25% $CaCO_3$) (Yang et al., 2017). The second group was also characterized by ∑REE < 250 ppm, but with greater MREE-enriched patterns and REEs mainly hosted in carbonate and organic fractions. The third group was characterized by ∑REE > 250 ppm, moderately enriched in MREE, and with REE mainly associated with carbonate, detrital apatite and siliciclastic minerals (Yang et al., 2017). Normalized to PAAS, the samples displayed distinct MREE-enrichment for the Hushpuckney, Stark, and Mulgrave shales (Yang et al., 2017).

Other samples did not display as prominent a fractionation pattern (Yang et al., 2017). Comparing enrichment patterns in various mineral fractions, Yang et al. (2017) determined that the carbonates show variability in MREE and HREE enrichment; HREE are preferentially hosted in siliciclastic minerals, whereas LREE preferentially occur (over MREEs and HREEs) in the organic fraction; and detrital apatite are MREE-enriched, although display low overall REE content.

The observed enrichment of HREE in the carbonate phases was attributed to HREE complexation in the pore waters from which the authigenic carbonates precipitated (Yang et al.,

2017). The LREE enrichment observed in the organic matter, however, was attributed to the preferential mobilization of HREE out of the organic matter during anoxic diagenesis which left behind a LREE-enriched remnant organic fraction (Yang et al., 2017). Yang et al. (2017) provide an in-depth description of the diagenetic cycling of REE, C and P.

Furthermore, studies by Yang et al. (2018) on the potential for REE to be released during the hydraulic fracturing of shales indicated variable dissolved ∑REE contents in hydraulic fracturing fluids from the Marcellus shale of the USA. During simulated fracturing conditions, the authors determined that REE in the shale phase were not effectively mobilized into the fracturing fluids, signifying that REE are not a significant byproduct of hydraulic fracturing processes (Yang et al., 2018).

An observed net loss in REE content of the fluids was attributed to either REE surface adsorption onto mineral phases due to an increase in PH during carbonate dissolution, or to incorporation into secondary clay minerals precipitating from solution (Yang et al., 2018). The authors also cautioned, however, that in the Marcellus shale samples studied, REE were mainly hosted in refractory mineral phases, and other black shale plays with higher REE concentrations and a larger extent of carbonate-hosted REE might more affectively mobilize REE during hydraulic fracturing processes (Yang et al., 2018).

REE distribution in oil shales were also studied by Cimen et al. (2013) and Berna (2019) for samples from Turkey, which range from Paleocene-Eocene and Middle-Late Miocene in age. Samples studied from the Celtek Formation yielded an average ∑REE of 345.3 ppm (ranging from 119.61 – 2057 ppm) with LREE enrichment, negative Ce and positive Eu anomalies (Berna, 2019). REE contents from oil shales of the Kızılçay Group displayed an average ∑REE of 50.68 ppm (ranging from 26.46 – 79.28 ppm), which is lower than that of the UCC, PAAS and NASC (Cimen et al., 2013).

Comparing the average ∑REE content of the oil shales to claystone (85.93 ppm) and marl (32.12 ppm), Cimen et al. (2013) theorized that REE (LREE in particular) are controlled by the clay fraction rather than by marl or the organic fraction. This was supported by a strong positive correlation between REE and SiO_2, Al_2O_3, Fe_2O_3, TiO_2 and K_2O, and a negative correlation with MgO and CaO (Cimen et al., 2013).

A decrease in REE with increasing carbonate content (Cimen et al., 2013) is however, contrary to findings by Yang et al. (2018) who reported an increase in REE concentration with increasing

carbonate content in oil shales from the Appalachian Basin, USA. In the Celtek Formation oil shales, HREE were more closely associated with organic material, pyrite and apatite (Cimen et al., 2013). Weakly negative Ce and weakly positive Eu anomalies were inferred by Cimen et al. (2013) to indicate a depositional environment characterized by reducing (low oxic-anoxic) conditions.

The study of REY distributions in shales overlying phosphorites in Egypt by Fakhry (1998) indicated that REY in the shales were post-depositionally remobilized and incorporated into the underlying phosphorite deposits. Where the average ∑REY concentration of the shales was 249.5 ppm, the underlying phosphorites were REY-enriched in comparison (average ∑REY = 945.1 ppm) (Fakhry, 1998). The presence of alternating REY-depleted shale layers (REY < 70 ppm) and REY-enriched layers (70 – 1123 ppm) indicated a pulsating process of diagenesis and REY-remobilization into the underlying phosphorites (Fakhry, 1998).

Shales in Russia from the Upper Jurassic to Lower Cretaceous Bazhenov Formation are considered the richest oil fields in West Siberia and are composed mainly of fine-grained carbonaceous clayey-siliceous rocks (Zanin et al., 2010). Zanin et al. (2010) determined the REE concentrations for the various lithologies within the formation and observed the following decreasing trend in average ∑REE concentrations: "phosphatic clayey-siliceous rocks (417.8 ppm) > argillites (140.4 ppm) > clayey-siliceous rocks (97.4 ppm) > silty argillites of anomalous member (84.66 ppm) > carbonates (26.0 ppm) > clayey-silty rocks anomalous member (21.2 ppm)" (Zanin et al., 2010; p. 366).

The phosphatic rocks of the Bazhenov Formation contained the highest concentrations of REE, followed by the clay fraction, as indicated by the REE-enriched argillites. Zanin et al. (2010) also observed an inverse relationship between REE content and TOC, indicating that REE in the Bazhenov area are controlled by clay minerals and not by the organic fraction. Additionally, LREE contents are controlled more by clays and partly by feldspars and apatite, whereas MREE and HREE concentrations are controlled more by apatite, pyrite and organic carbon (Zanin et al., 2010).

Mineral composition rather than rates of sedimentation or redox conditions was inferred to be the controlling factor on REE concentration, based on the high concentration of REE in clay-rich argillites which would have been deposited as turbidites under quick sedimentation rates (Zanin et al., 2010). An absence of a negative Ce anomaly and both positive and negative Eu anomalies was attributed to varying redox conditions between the samples (Zanin et al., 2010).

In Canada, shales have also been studied for REE content by Turner (2015) and Goodarzi and Gentzis (2018). Turner (2015) reported the presence of a >20 m-thick black shale interval in the Cambrian Hess River Formation in the Misty Creek Embayment (NWT) with elevated contents of base metals (values not reported) as well as Ba. Although the author reports that ∑REE concentrations roughly increase up section, they were not particularly correlative to calcite or phyllosilicate minerals. Relative enrichment patterns indicate slight LREE-enrichment relative to MREE, but slight MREE depletion relative to HREE (Turner, 2015).

Where moderate to significant positive Eu anomalies were inferred to be caused by hydrothermal venting, negative Y anomalies and weakly positive Ce anomalies indicated mild anoxia (Turner, 2015). The shales also displayed no or only weakly positive La and Gd anomalies. In their studies of Devonian carbonaceous shales and coals in the Arctic, Goodarzi and Gentzis (2018) determined that REE contents were higher in the coals (48.14 – 97.04 ppm) relative to the shales (31.46 ppm), and all samples were LREE-enriched relative to HREE.

Soil analyses of gray and black shales in the USA carried out by Ma et al. (2011) and Jin et al. (2017) also provide important information on REE fractionation during weathering of shales. REE contents in solid samples (bedrock, regolith, stream sediments) as well as in natural waters (pore waters and streams) were investigated, with results indicating that chemical leaching of organic-rich and acidic soils results in REE depletion (Ma et al., 2011). Ma et al. (2011) proposed that varying degrees of REE-depletion are controlled by different rates of chemical weathering and surface erosion, which in turn are controlled by different microclimate conditions.

Furthermore, MREE are preferentially released from rhabdophane, resulting in a preferential removal of MREE (up to 22% more) over LREE and HREE during weathering. Strong positive Ce anomalies of the solid samples indicated a preferential precipitation of Ce under oxidizing conditions during the release, transport and redistribution of REE (Ma et al., 2011). Positive Eu anomalies in the natural waters, however, were attributed to the weathering of plagioclase in the shale bedrock (Ma et al., 2011).

Under the same climate conditions, black shales weather faster and release greater concentrations of REE than do grey shales; this is attributed to the higher content of organic matter and sulphides in black shale relative to grey shale, as well as a lower soil PH (Jin et al., 2017). REE are initially released quickly from REE-bearing phases in the shale (phosphates, sulphides and organic matter), followed by a slower release during the dissolution of clay minerals (Jin et

al., 2017). The mobilized REE are then re-adsorbed onto mineral surfaces at depth with an increase in pH and dissolved organic matter, and a decrease in REE solubility (Jin et al., 2017). Therefore, soils are generally REE-depleted at shallow depths, but REE-enriched at depth (Jin et al., 2017).

Table 5. *∑REE (or REY, if data includes Y) contents of various shale deposits.*

Region	Sample	∑REE Avg (ppm)	∑REE Range (ppm)	Reference
World	Worldwide black shales	134.19	Not reported	Ketris and Yudovich (2009)
China	Haudian lacustrine oil shales	153.8	57.3 – 245.3	Bai et al. (2011)
China	Changshe Mountain marine oil shales	68.2	13.1 – 118.4	Fu et al. (2010)
China	Lacustrine shales from the Shengli River area	53.1	46.8 – 67.9	Fu et al. (2011)
China	Oil shale samples from three provinces	171.2	57.3 – 318.3	Wang et al. (2014)
USA	Green River shales (Colorado, Utah)	98.9 (REY)	66.3 – 141.3 (REY)	Birdwell (2012)
USA	Java and Huron marine shales	168.0	114.1 – 233.3	Lev and Filer (2004)
USA	Marcellus Shale	202.2 (REY)	72.2 – 278.8 (REY)	Noack et al. (2015)
USA	Marcellus, West Virginia shales	227.4 (REY)	131.7 – 402.2 (REY)	Phan et al. (2019)
USA	Hydraulic fracturing fluids from the Marcellus shale	Not reported	145 – 170	Yang et al. (2018)
USA	Hushpuckney and Stark shales	Not reported	280 – 380	Yang et al. (2018)
USA	Woodford shale	77	Not reported	Yang et al. (2018)
Turkey	Oil shale samples from the Celtek Fm	345.3	119.6 – 2058	Berna (2019)
Turkey	Oil shales from the Kızılçay Group	50.7	26.5 – 79.3	Cimen et al. (2013)
Egypt	Dakhla Shale	249.5 (REY)	50.8 – 1123 (REY)	Fakhry et al. (1998)
Egypt	Phosphorites underlying Dakhla Shale	945.1 (REY)	194.9 – 1349 (REY)	Fakhry et al. (1998)
Russia	Bazhenov Fm (phosphatic clayey-siliceous)	417.8	301.7 – 534.0	Zanin et al. (2010)
Russia	Bazhenov Fm (argillite)	140.4	60.2 – 197.3	Zanin et al. (2010)
Russia	Bazhenov Fm (clayey-siliceous)	97.4	9.4 – 176.7	Zanin et al. (2010)
Russia	Bazhenov Fm (silty argillites)	84.7	N/A (n=1)	Zanin et al. (2010)
Russia	Bazhenov Fm (carbonates)	26.1	11.4 – 40.7	Zanin et al. (2010)
Russia	Bazhenov Fm (clayey-silty, anomalous member)	21.2	18.9 – 23.5	Zanin et al. (2010)

Region	Sample	∑REE Avg (ppm)	∑REE Range (ppm)	Reference
Canada	Carbonaceous shales	31.46	Not reported	Goodarzi and Gentzis (2018)

3. REY in Canadian Shale Deposits

All the bulk REY (La, Ce, Pr, Nd, Sm, Eu, Gd, Tb, Dy, Ho, Er, Tm, Yb, Lu, and Y) concentrations were determined using ICP-MS at Acme Laboratories in Vancouver, and data variability was checked by international standards and analysis of replicate samples (analytical precision and accuracy are within 10% for all samples). Samples were digested using a combination of high purity acids (HF, HNO_3, $HClO_4$, HCl). Precision and accuracy for Mo concentrations were determined using the reference standard OREAS 45e, prepared from a lateritic soil from Western Australia, as well as random duplicate analysis of sample splits (precision and accuracy are within 5% for random splits).

The REY raw and normalized data for select Canadian fine-grained siliciclastic sedimentary rock, dominantly organic-rich shales are presented in Table 6A and 6B, respectively. The range of REE concentration as well as the mean values of each sedimentary unit presented in Figure 8. The data is from the Geological Survey of Canada in Calgary and includes both raw and UCC-normalized data for the Gordondale Member, Duvernay Formation, Utica Formation, Garbutt Formation, Besa River Formation, Montney Formation, Kanguk Formation, and the Second White Specks Formation.

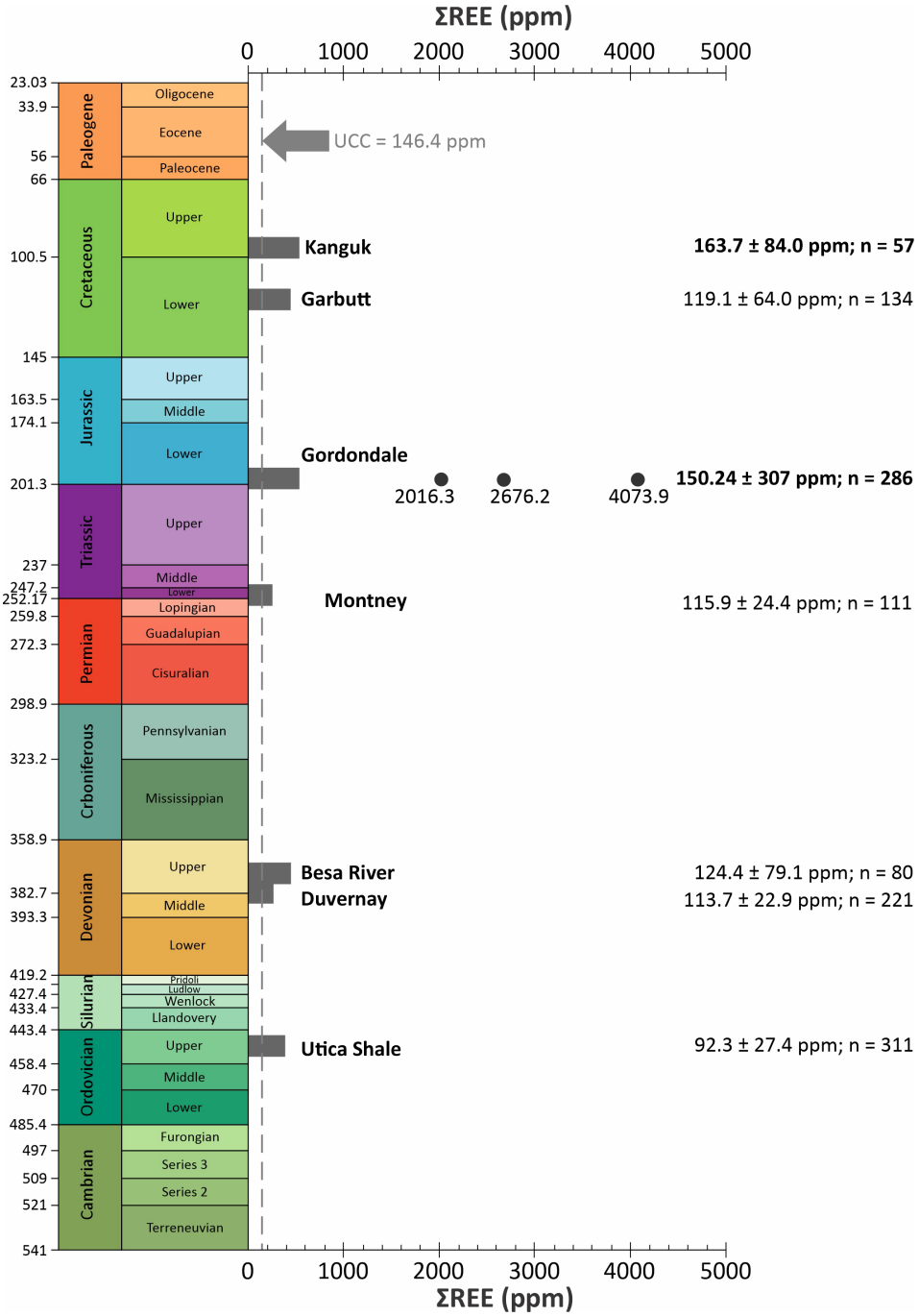

Figure 8. *Distribution of studied major Canadian organic-rich shales throughout Phanerozoic. Gray horizontal bars for each sedimentary unit show the range of ΣREE variations, individual filled circles show the extreme values of some organic-rich shales. The mean and standard deviation and number of samples for each unit provided. The gray broken line shows the ΣREE of the upper continental crust (UCC).*

Table 6A: *Summary statistics of REY data for select Canadian deposits. (Data gathered from the Geological Survey of Canada, Calgary).*

Formation	Sample Set	# Samples	∑REE (Mean)	∑REY			∑LREE (Mean)	∑HREE (Mean)	LREE/HREE (Mean)	C_{outl} (Mean)	$C_{def,rel}$ (Mean)
				Mean	Max	Min					
Gordondale	11-19	131	134.3	178.8	2942.9	14.4	109.5	24.8	4.7	2.0	47.6
	16-5	155	163.7	213.2	5150.9	8.5	136.6	27.1	5.3	1.7	44.9
	All samples	*286*	*150.2*	*197.5*	*5150.9*	*8.5*	*124.2*	*26.1*	*5.1*	*1.8*	*46.2*
Duvernay	Fox Creek	16	125.5	149.3	236.9	120.3	112.0	13.5	8.4	1.1	36.2
	Kaybob	105	107.7	129.7	171.7	60.4	95.8	12.0	8.0	1.1	38.4
	All samples	*121*	*113.7*	*135.0*	*239.0*	*60.4*	*101.5*	*12.2*	*8.4*	*1.1*	*36.7*
Utica	St. Augustin No. 1A	43	93.9	105.3	160.8	17.5	86.0	7.9	10.9	0.8	30.5
	Becancour No. 8	57	97.7	111.7	193.9	32.0	88.6	9.1	9.6	0.8	32.7
	St. Edouard No. 1	209	90.3	104.8	342.5	48.1	80.8	9.5	8.5	0.9	33.7
	All samples	*309*	*92.2*	*106.2*	*342.5*	*17.5*	*83.0*	*9.2*	*9.0*	*0.9*	*33.1*
Garbutt	K-32-060-10-123-15	17	105.6	122.9	181.8	65.8	89.5	16.1	5.5	1.0	38.1
	Liard A01	13	105.0	120.4	146.9	104.1	90.8	14.2	6.4	1.0	36.4
	WA9950	18	202.9	234.0	342.1	73.3	180.0	22.9	7.9	0.9	34.8
	WA9941	19	59.0	70.8	141.7	32.6	47.9	11.1	4.3	1.2	41.4
	WA18890	21	138.0	164.8	203.8	128.6	117.8	20.3	5.9	1.1	38.7
	WA14517	12	141.1	159.3	239.0	91.5	127.1	14.0	9.5	0.8	32.4
	WA6468	22	77.5	92.2	271.9	30.4	64.6	12.9	4.5	1.1	39.7
	WA6477	5	190.3	229.3	454.9	130.3	159.3	31.0	5.6	1.2	40.1
	WA13960	7	111.8	134.1	281.9	83.6	92.4	19.4	4.9	1.0	38.2
	All samples	*134*	*119.1*	*139.5*	*454.9*	*30.4*	*102.3*	*16.8*	*6.0*	*1.0*	*37.9*
Besa River	WA1331	50	160.6	186.2	500.0	83.9	143.3	17.3	12.1	1.2	34.9
	WA21755	4	189.6	213.3	310.3	166.9	171.6	18.1	10.1	0.8	31.9
	WA2563	26	44.7	56.0	78.3	35.6	38.0	6.7	5.7	1.6	44.1
	All samples	*80*	*124.4*	*145.3*	*500.0*	*35.6*	*110.5*	*13.9*	*10.0*	*1.3*	*37.7*
Montney	1 (1-28-70-9W6)	13	93.8	106.8	137.0	77.1	82.9	10.9	7.6	1.0	36.3
	2 (B-35-G/93-P-01)	17	121.5	138.3	204.7	88.0	109.1	12.4	8.8	1.0	34.5
	6 (C-81-j/93-P-7 PSP)	7	112.8	133.1	149.3	117.3	98.8	14.0	7.2	1.1	38.5
	21 (b-52-I/93-P-6)	8	136.5	159.5	196.6	123.1	120.7	15.8	7.7	1.1	36.9
	28 (14-13-78-16W6)	12	121.8	140.4	157.8	98.9	108.1	13.7	7.9	1.0	36.3
	31 (4-19-77-10W6)	7	145.5	162.2	176.5	150.2	131.7	13.8	9.6	0.9	32.5
	34 (141258 CMS)	22	96.4	110.8	144.0	61.3	85.0	11.5	7.4	1.1	37.1
	50 (16-29-69-10W6)	5	115.3	131.3	153.5	109.0	102.6	12.7	8.1	1.0	36.6
	51 (SP)	9	117.4	135.6	169.5	80.7	104.2	13.2	7.9	1.0	35.8
	58 (7-34-78-11W6)	3	138.2	156.0	161.4	148.6	124.4	13.8	9.0	0.9	32.8
	59 (6-14-78-11W6)	4	127.8	145.5	168.1	110.1	114.4	13.4	8.6	0.9	34.4
	60 (15-30-77-10W6)	4	135.4	152.8	174.3	103.5	121.6	13.8	8.7	0.9	33.0
	All samples	*111*	*115.9*	*132.8*	*204.7*	*61.3*	*103.1*	*12.8*	*8.0*	*1.0*	*35.8*
Kanguk	Axel Heiberg Island	13	194.1	216.0	347.5	92.0	174.3	19.8	9.3	0.7	30.7
	Banks Island	31	148.3	167.3	492.8	74.2	133.1	15.2	9.8	0.8	31.7
	Banks Island - Sachs River	6	137.0	162.9	216.7	101.5	115.3	21.7	5.4	1.1	38.6
	Banks Island Bentonite	8	191.7	221.3	480.4	109.6	168.3	23.4	8.3	1.1	37.7

	All samples	*58*	*163.6*	*185.5*	*492.8*	*74.2*	*145.6*	*18.1*	*9.0*	*0.9*	*33.0*
Second White Specks	7-29-42-12 (2WS)	8	118.1	136.8	238.5	82.9	105.0	13.1	8.2	0.9	33.7
	7-29-42-12 (Belle Fourche)	3	119.2	137.6	139.9	136.3	104.0	15.2	6.9	0.9	34.5
	All samples	*11*	*118.4*	*137.0*	*238.5*	*82.9*	*104.7*	*13.7*	*7.9*	*0.9*	*33.9*

Table 6B: *Summary statistics of REY upper continental crust (UCC) and calculated anomalies for select Canadian deposits. (Data gathered from the Geological Survey of Canada, Calgary).*

Formation	Sample Set	# Samples	$\sum LREE_N$ (Mean)	$\sum HREE_N$ (Mean)	$LREE_N/HREE_N$ (Mean)	Eu_N/Eu_N^* (Mean)	Ce_N/Ce_N^* (Mean)	Gd_N/Gd_N^* (Mean)	La_N/La_N^* (Mean)	La_N/Sm_N (Mean)	La_N/Yb_N (Mean)	La_N/Lu_N (Mean)	Gd_N/Lu_N (Mean)	Gd_N/Yb_N (Mean)	Ce_N/Yb_N (Mean)
Gordondale	11-19	131	5.1	14.5	0.4	1.0	0.7	1.2	1.7	0.6	0.6	0.6	1.3	1.2	0.5
	16-5	155	6.2	16.0	0.4	1.1	0.7	1.1	1.2	0.7	0.7	0.7	1.2	1.2	0.5
	All samples	*286*	*5.7*	*15.3*	*0.4*	*1.0*	*0.7*	*1.2*	*1.4*	*0.7*	*0.7*	*0.7*	*1.2*	*1.2*	*0.5*
Duvernay	Fox Creek	16	4.3	7.2	0.6	1.1	0.8	1.2	1.2	1.0	1.4	1.5	1.6	1.5	1.1
	Kaybob	105	3.9	6.9	0.6	1.0	0.8	1.2	1.2	0.9	1.2	1.3	1.6	1.5	1.0
	All samples	*121*	*4.1*	*7.0*	*0.6*	*1.1*	*0.8*	*1.2*	*1.2*	*0.9*	*1.3*	*1.4*	*1.6*	*1.5*	*1.0*
Utica	St. Augustin No. 1A	43	5.0	6.4	0.8	1.2	0.9	1.2	0.9	1.3	1.6	1.8	1.1	1.0	1.5
	Becancour No. 8	57	3.4	5.4	0.6	1.0	1.0	1.3	1.2	1.1	1.2	1.3	1.3	1.2	1.2
	St. Edouard No. 1	209	3.1	5.5	0.6	1.0	1.0	1.1	1.2	1.0	1.1	1.3	1.5	1.3	1.1
	All samples	*309*	*3.2*	*5.4*	*0.6*	*1.0*	*1.0*	*1.2*	*1.2*	*1.0*	*1.2*	*1.3*	*1.4*	*1.3*	*1.1*
Garbutt	K-32-060-10-123-15	17	3.8	9.8	0.4	1.1	1.0	1.1	0.8	0.6	0.5	0.5	0.9	1.0	0.6
	Liard A01	13	3.8	8.6	0.4	1.1	1.0	1.1	1.0	0.6	0.6	0.6	1.0	1.0	0.7
	WA9950	18	7.3	14.1	0.5	1.2	0.9	1.0	0.9	0.8	0.9	0.8	1.0	1.1	0.9
	WA9941	19	2.1	6.7	0.3	1.0	1.0	1.2	1.1	0.5	0.4	0.4	0.9	0.9	0.4
	WA18890	21	5.0	12.5	0.4	1.2	0.9	1.0	0.8	0.7	0.7	0.6	1.0	1.1	0.7
	WA14517	12	5.0	8.3	0.6	1.0	0.9	1.0	0.9	0.9	1.3	1.1	1.1	1.3	1.2
	WA6468	22	2.7	7.8	0.3	1.0	1.0	1.2	1.1	0.5	0.4	0.4	0.8	0.8	0.4
	WA6477	5	7.0	18.0	0.4	1.0	1.0	1.0	0.9	0.5	0.6	0.6	1.2	1.3	0.7
	WA13960	7	3.9	11.8	0.3	1.0	1.1	1.1	0.9	0.6	0.4	0.4	0.8	0.9	0.5
	All samples	*134*	*4.3*	*10.2*	*0.4*	*1.1*	*1.0*	*1.1*	*0.9*	*0.6*	*0.6*	*0.6*	*1.0*	*1.0*	*0.7*
Besa River	WA1331	50	6.4	9.8	0.9	1.2	0.7	1.0	0.9	0.9	3.2	3.8	3.7	3.1	2.3
	WA21755	4	7.0	10.7	0.7	1.1	0.9	1.0	0.8	0.8	1.5	1.4	1.6	1.7	1.5
	WA2563	26	1.8	3.8	0.5	1.1	0.7	1.2	1.1	0.6	0.9	1.2	2.3	1.7	0.7
	All samples	*80*	*4.9*	*7.9*	*0.8*	*1.1*	*0.7*	*1.1*	*0.9*	*0.8*	*2.3*	*2.8*	*3.1*	*2.6*	*1.7*
Montney	1 (1-28-70-9W6)	13	3.6	6.3	0.6	1.1	0.9	1.2	1.1	0.6	1.0	1.1	1.8	1.7	1.0
	2 (B-35-G/93-P-01)	17	4.5	7.0	0.6	1.0	0.8	1.3	1.1	0.8	1.4	1.5	1.8	1.7	1.2
	6 (C-81-j/93-P-7 PSP)	7	4.2	7.9	0.5	1.1	0.9	1.1	1.0	0.7	1.0	1.1	1.8	1.6	0.9
	21 (b-52-I/93-P-6)	8	5.0	9.0	0.6	1.0	0.8	1.1	1.1	0.8	1.2	1.4	1.7	1.5	1.0
	28 (14-13-78-16W6)	12	4.5	7.9	0.6	1.0	0.9	1.2	1.2	0.7	1.1	1.2	1.7	1.5	1.0
	31 (4-19-77-10W6)	7	5.4	7.9	0.7	1.0	0.9	1.2	1.2	0.8	1.4	1.6	1.8	1.6	1.2
	34 (141258 CMS)	22	3.6	6.5	0.6	1.1	0.9	1.2	1.5	0.6	1.0	1.2	2.0	1.7	1.0
	50 (16-29-69-10W6)	5	4.3	7.0	0.6	1.0	0.9	1.3	1.4	0.7	1.2	1.4	2.1	1.8	1.2
	51 (SP)	9	4.3	7.4	0.6	1.0	0.8	1.2	1.1	0.9	1.2	1.4	1.8	1.5	1.0
	58 (7-34-78-11W6)	3	5.0	8.1	0.6	1.0	0.9	1.2	1.1	0.9	1.3	1.1	1.2	1.4	1.1
	59 (6-14-78-11W6)	4	4.7	7.9	0.6	1.2	0.9	1.2	1.1	0.9	1.3	1.2	1.4	1.6	1.1
	60 (15-30-77-10W6)	4	4.8	8.2	0.6	1.1	0.9	1.2	1.1	0.9	1.4	1.1	1.3	1.6	1.2
	All samples	*111*	*4.3*	*7.3*	*0.6*	*1.0*	*0.9*	*1.2*	*1.2*	*0.7*	*1.2*	*1.3*	*1.8*	*1.6*	*1.1*
Kanguk	Axel Heiberg Island	13	6.8	11.7	0.6	0.9	1.0	1.1	0.8	0.9	1.0	1.1	1.2	1.1	1.1
	Banks Island	31	5.3	9.2	0.6	1.0	0.9	1.2	1.0	0.9	1.3	1.3	1.2	1.3	1.2
	Banks Island - Sachs River	6	4.9	13.1	0.4	0.9	1.0	1.1	0.8	0.6	0.5	0.4	0.8	1.0	0.6
	Banks Island Bentonite	8	5.8	15.1	0.4	0.8	-	1.1	-	-	-	-	1.4	1.4	1.2
	All samples	*58*	*5.7*	*11.0*	*0.6*	*1.0*	*0.9*	*1.1*	*1.0*	*0.9*	*1.2*	*1.1*	*1.2*	*1.2*	*1.1*
Second White Specks	7-29-42-12 (2WS)	8	4.2	7.9	0.5	1.2	0.8	1.2	1.0	1.0	1.1	1.0	1.0	1.1	0.9
	7-29-42-12 (Belle Fourche)	3	4.2	9.2	0.5	1.0	0.9	1.2	0.8	0.9	0.7	0.7	0.9	1.0	0.7
	All samples	*11*	*4.2*	*8.2*	*0.5*	*1.1*	*0.9*	*1.2*	*1.0*	*1.0*	*1.0*	*0.9*	*1.0*	*1.1*	*0.8*

3.1 Gordondale Member

Samples from the Lower Jurassic Gordondale Member of the Fernie Formation are composed of shale and were retrieved from two wells in west-central Alberta: well 11-19 (1845 to 1871 m depth) and well 16-05 (2622.03 to 2646.63 m depth). Average ∑REY concentrations for the wells are 178.8 ppm (range: 14.4 – 2942.9 ppm) and 213.2 ppm (range: 8.5 – 5151 ppm) respectively, which are higher than worldwide black shales (134.2 ppm; Ketris and Yudovich, 2009), the UCC (168.4 ppm; Taylor and McLennon, 1985), the NASC (165.4 ppm; Gromet et al., 1984), world coal (68.5 ppm; Ketris and Yudovich, 2009), Chinese coal (137.9 ppm; Dai et al., 2008) and USA coal (62.1 ppm; Finkelman, 1993).

REY concentration does not appear to correspond with TOC or vary significantly with depth. According to Seredin and Dai's (2012) classification based on the outlook coefficient, samples from the 16-05 well have promising REY concentrations (mean C_{outl} = 1.72), whereas samples from well 11-19 (mean C_{outl} = 1.96) are promising to highly promising in terms of economic viability (Fig. 9). Normalized to the UCC, the Gordondale samples exhibit weak positive Eu anomalies and distinct negative Ce anomalies (Fig. 10). The samples display M-type (La_N/Sm_N < 1, Gd_N/Lu_N >1) to H-type (La_N/Lu_N < 1) distribution as classified by Seredin and Dai (2012).

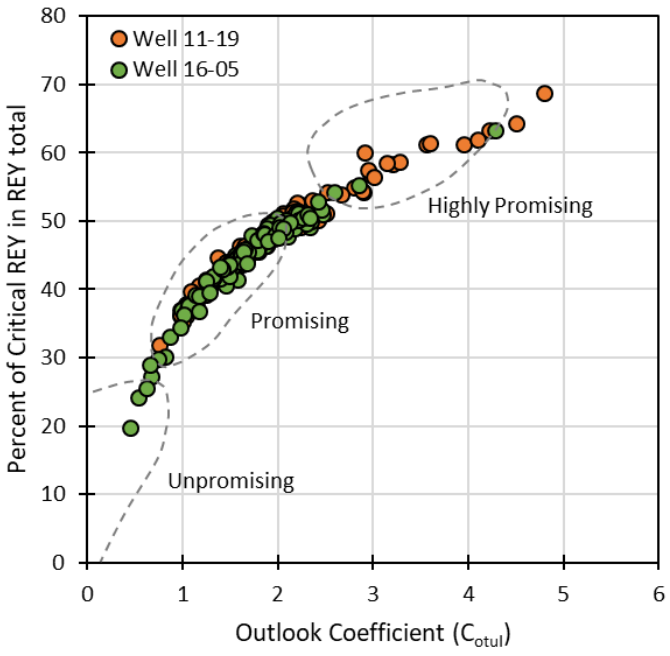

Figure 9. *(A) REY classification of the Gordondale Member samples (modified after Seredin and Dai, 2012).*

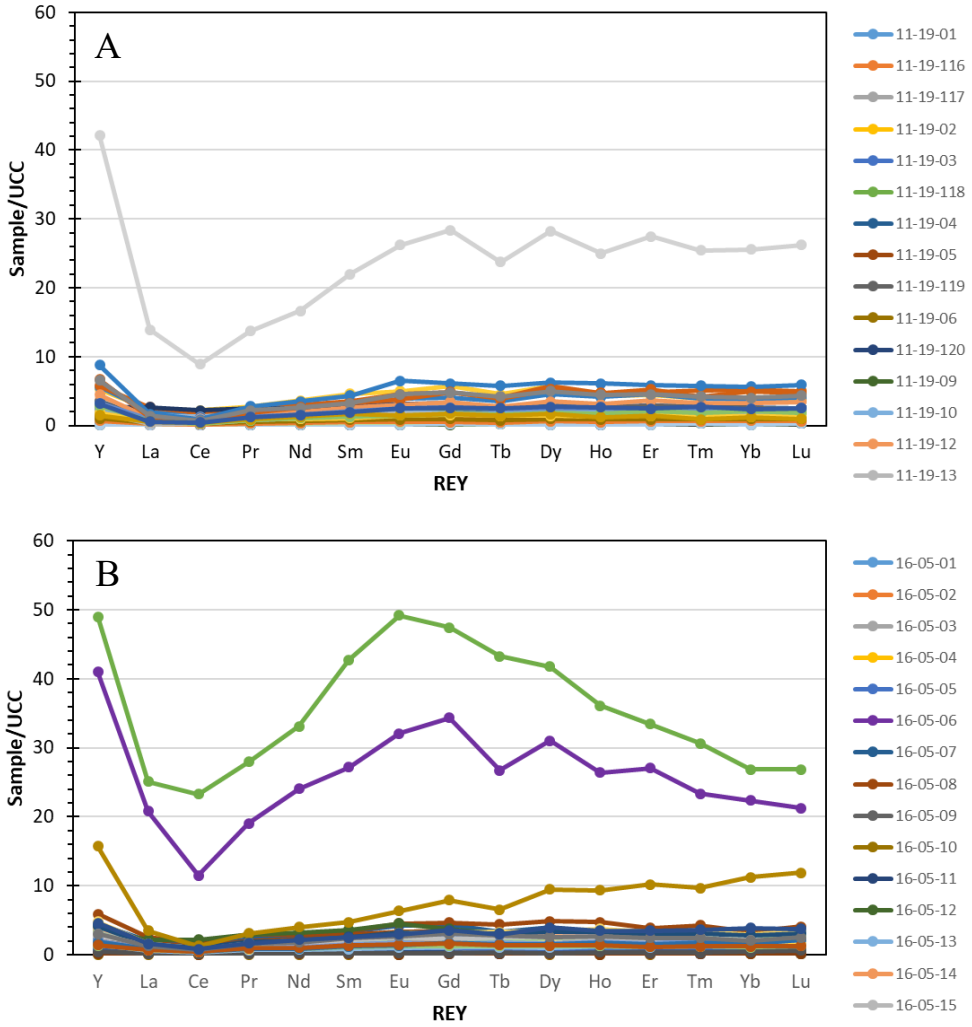

Figure 10. *UCC-normalized REE distribution patterns for Gordondale Formation samples from (A) well 11-19 and (B) well 16-05.*

3.2 Duvernay Formation

Samples from the Devonian Duvernay Formation are composed of shale and were retrieved from a well in Fox Creek (2989.3 to 3035 m depth) and a well in Kaybob (3340 to 3387.6 m depth), west-central Alberta. Average ∑REY concentrations are 149.4 ppm (range: 120.3 – 236.9 ppm) and 129.9 ppm (range: 60.4 – 171.7 ppm) respectively, which are slightly higher than worldwide black shales (134.2 ppm; Ketris and Yudovich, 2009) and Chinese coal (137.9 ppm; Dai et al., 2008) and significantly higher than world coal (68.5 ppm; Ketris and Yudovich, 2009) and USA

coal (62.1 ppm; Finkelman, 1993), but lower than the UCC (168.4 ppm; Taylor and McLennon, 1985) and the NASC (165.4 ppm; Gromet et al., 1984).

According to Seredin and Dai's (2012) classification based on the outlook coefficient, all samples (from both Fox Creek and Kaybob) exhibit promising REY concentrations in terms of economic viability (Fig. 11). Normalized to the UCC, the Duvernay samples exhibit weak positive Eu anomalies and negative Ce anomalies (Fig. 12). The samples display M-type ($La_N/Sm_N < 1$, $Gd_N/Lu_N > 1$) distribution as classified by Seredin and Dai (2012). In the Fox Creek well, a three meter zone (3004 to 3007 m) has a higher REY content (roughly 150 – 250 ppm) than the remainder of the well (roughly 100 – 150 ppm). Contrarily, the four deepest samples (< 3028 m) present the lowest REY concentrations at < 100 ppm. In the Kaybob well, REY content roughly increases up-section.

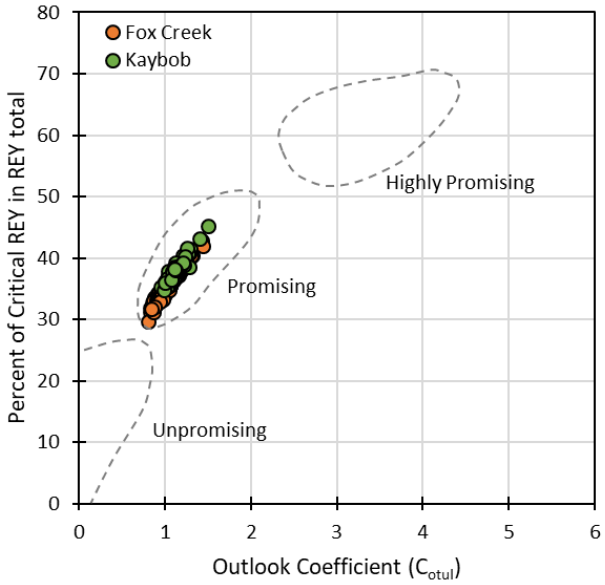

Figure 11. *REY classification of the Duvernay Formation samples (modified after Seredin and Dai, 2012).*

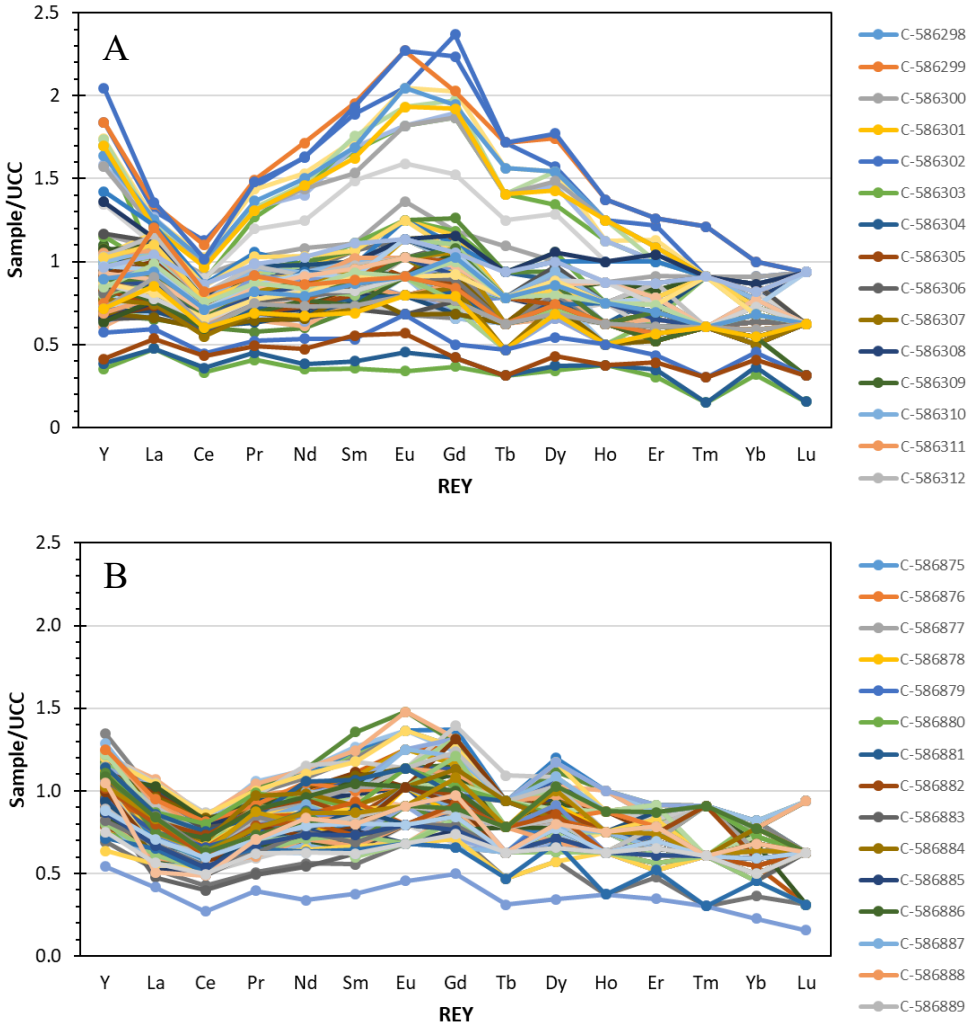

Figure 12. *UCC-normalized REE distribution patterns for Duvernay Formation samples from (A) the Fox Creek well and (B) the Kaybob well.*

3.3 Utica Formation

Samples from the Upper Ordovician Utica Formation are composed of shale and were retrieved from three wells in Quebec: St. Augustine (420.15 to 514.00m depth), Becancour (700.15 to 751.65m depth) and St. Edouard (1997.88 to 2030.45m depth). Average ∑REY concentrations are 105.3 ppm (range: 17.5 –160.8 ppm), 111.7 ppm (range: 32.0 – 193.9 ppm) and 104.8 ppm (range: 48.1 – 342.5 ppm), respectively (for a total ∑REY concentrations for all samples of 106.2 ppm) (Fig. 13).

The average REY content of these samples is therefore lower than worldwide black shales (134.2 ppm; Ketris and Yudovich, 2009), the UCC (168.4 ppm; Taylor and McLennon, 1985), the NASC (165.4 ppm; Gromet et al., 1984) and Chinese coal (137.9 ppm; Dai et al., 2008), but higher

than world coal (68.5 ppm; Ketris and Yudovich, 2009) and USA coal (62.1 ppm; Finkelman, 1993). According to Seredin and Dai's (2012) classification based on the outlook coefficient, the samples are mainly in the promising range in terms of economic viability (Fig. 13). Mean C_{outl} values are 0.77, 0.84 and 0.88 for the St. Augustine, Becancour and St. Edouard samples, respectively. Normalized to the UCC, the St. Augustine and Becancour samples exhibit weak positive Eu anomalies whereas the St. Edouard samples display weak negative Eu anomalies (Fig. 14). All samples display weak negative Ce anomalies. The samples display mainly L-type (La_N/Lu_N > 1) distribution as classified by Seredin and Dai (2012), with St. Edouard samples displaying L- to M-type distribution (Fig. 13).

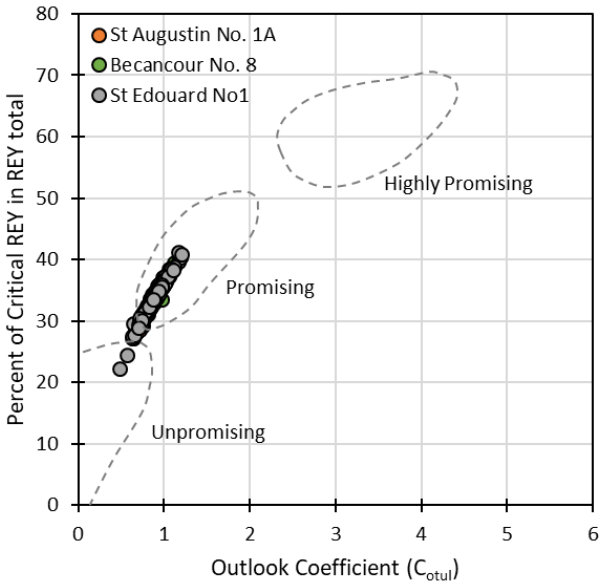

Figure 13. *REY classification of the Utica Formation samples (modified after Seredin and Dai, 2012).*

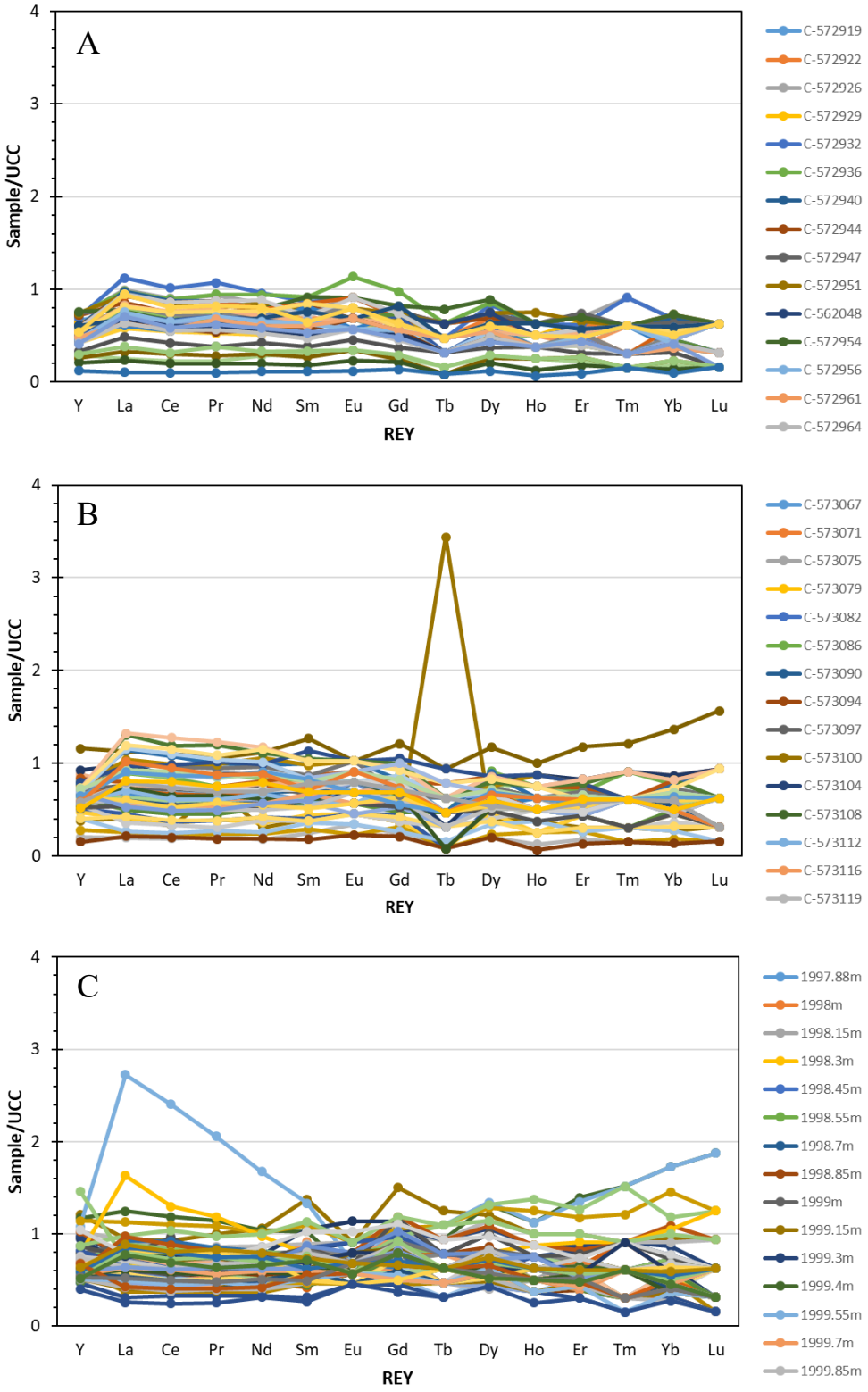

Figure 14. *UCC-normalized REE distribution patterns of the Utica Formation samples from (A) St. Augustin, (B) Becancour, and (C) St. Edouard.*

3.4 Garbutt Formation

Samples from the lower Cretaceous Garbutt Formation are composed of shale and were retrieved from 8 wells in the Liard Basin, British Columbia. The average ∑REY concentration for all samples is 139.5 ppm (range: 30.4 – 454.9 ppm), which is comparable to worldwide black shales (134.2 ppm; Ketris and Yudovich, 2009), but lower than the UCC (168.4 ppm; Taylor and McLennon, 1985), the NASC (165.4 ppm; Gromet et al., 1984) and Chinese coal (137.9 ppm; Dai et al., 2008); and higher than world coal (68.5 ppm; Ketris and Yudovich, 2009) and USA coal (62.1 ppm; Finkelman, 1993).

According to Seredin and Dai's (2012) classification based on the outlook coefficient, the samples have mainly promising REY concentrations (mean C_{outl} = 1.05) in terms of economic viability of Garbutt Formation in Liard (Fig. 15A) and Horn River (15B) basins. Normalized to the UCC, the samples mainly exhibit weak positive Eu anomalies (with two wells having weak negative anomalies) and weak negative Ce anomalies (Figs. 16 and 17). The samples mainly display H-type ($La_N/Lu_N < 1$) distribution with some M-type ($La_N/Sm_N < 1$, $Gd_N/Lu_N > 1$) as classified by Seredin and Dai (2012).

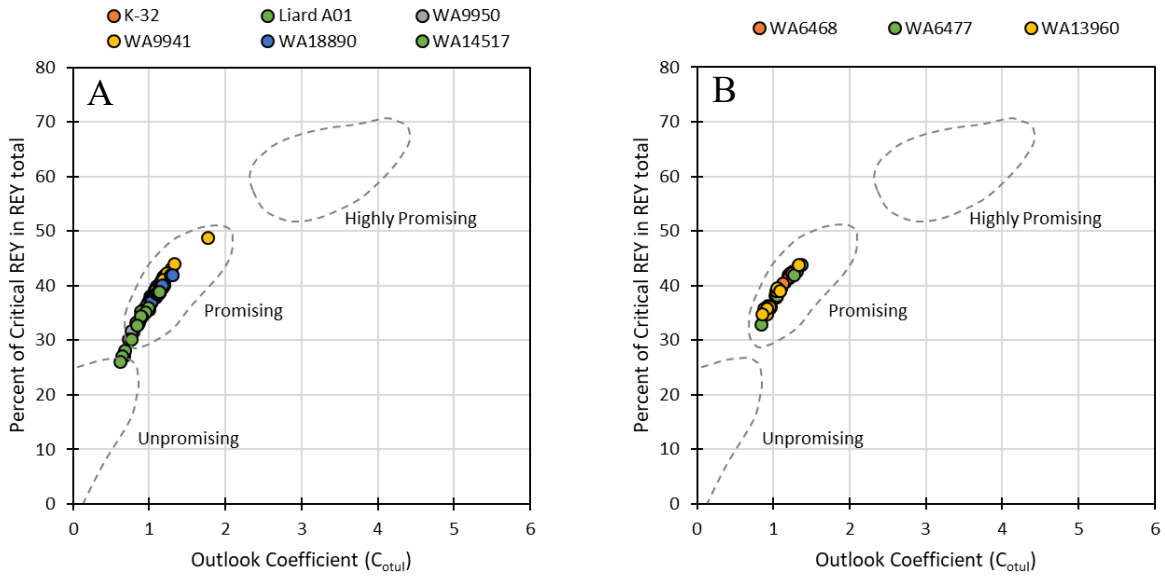

Figure 15. *(A) REY classification of the Garbutt Formation samples (modified after Seredin and Dai, 2012).*

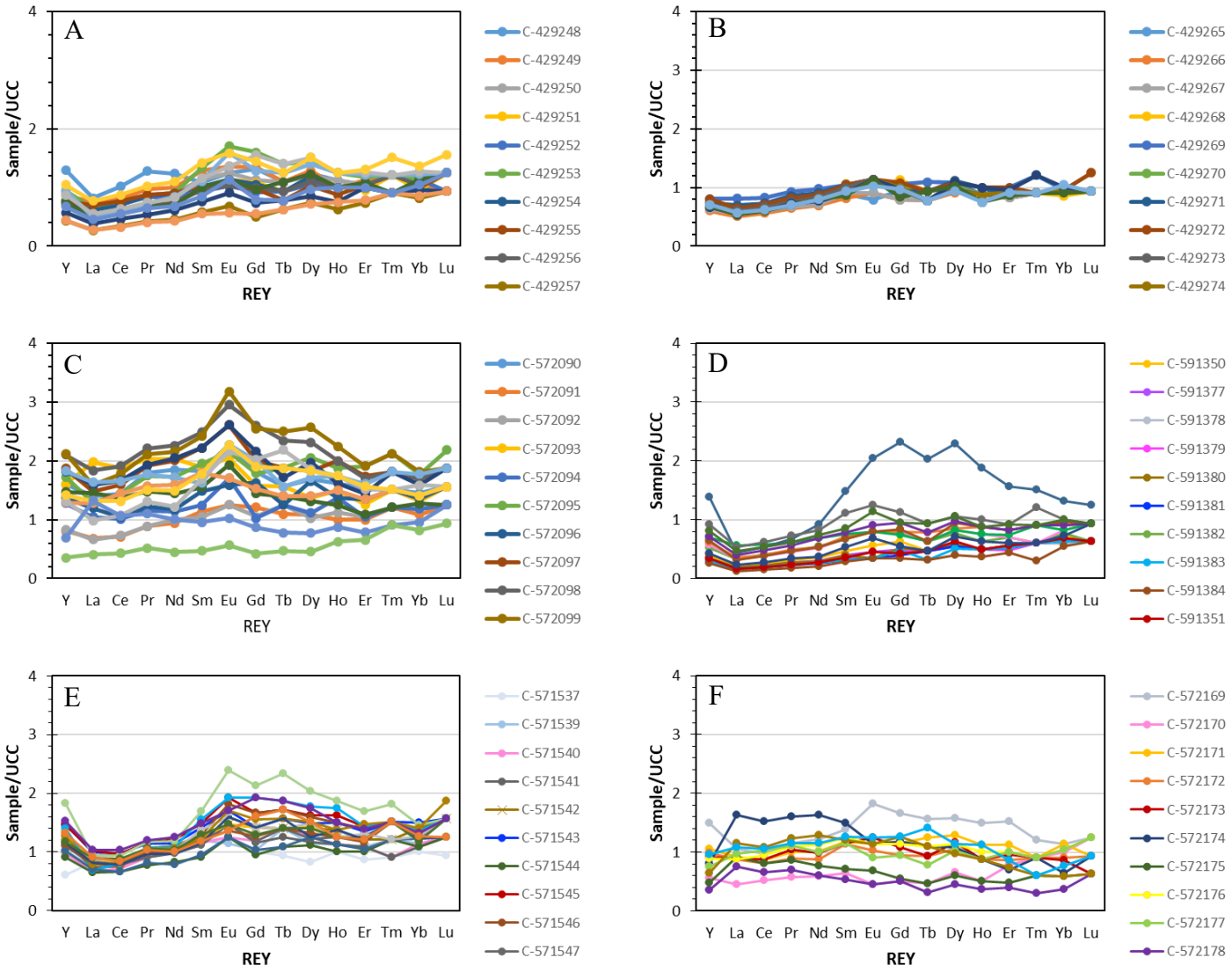

Figure 16. *UCC-normalized REE distribution patterns of the Garbutt Formation samples in Liard Basin from wells (A) K-32, (B) Liard A01, (C) WA9950, (D) WA9941, (E) WA18890, (F) WA14517.*

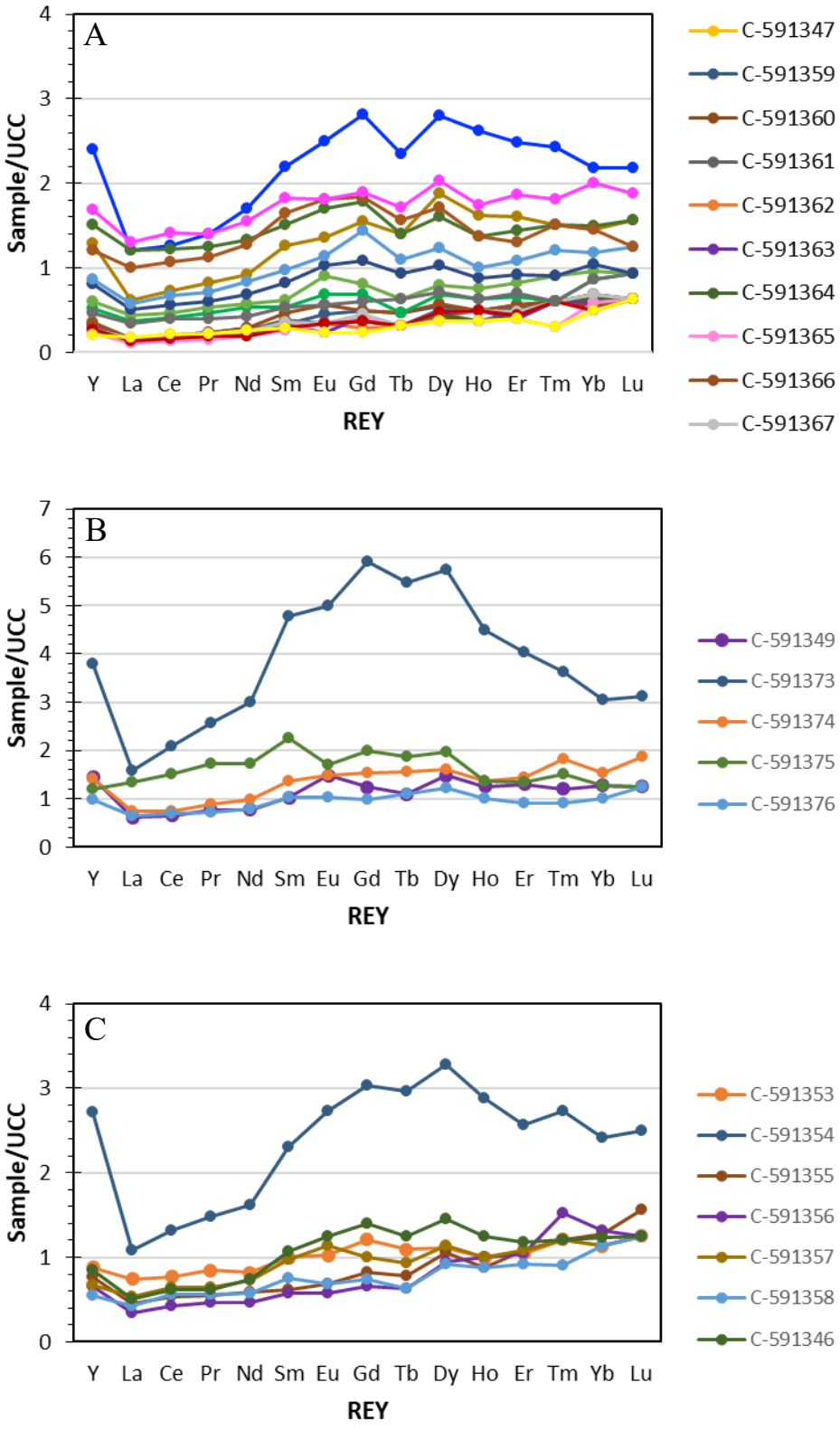

Figure 17. *UCC-normalized REE distribution patterns of the Horn River Basin Garbutt Formation samples from wells (A) WA6468, (B) WA6477, and (C) WA13960.*

3.5 Besa River Formation

Samples from the Devonian Besa River Formation are composed of shale and were retrieved from three wells in British Columbia: WA1331 (3688.99 to 3895.20m depth), WA21755 (1856.00 to 2114.00m depth) and WA2563 (3778.00 to 3785.62m depth). The average ∑REY concentrations for all samples is 145.26 ppm (range: 35.6 – 500.0 ppm); where wells WA1331 and WA21755 have average ∑REY concentrations of 186.2 ppm and 213.3 ppm respectively, however, well WA2563 is REY-depleted with an average ∑REY concentration of 56.0 ppm.

This well has a lower average ∑REY content than the reference standards, whereas the other wells have average ∑REY contents greater than the standards (worldwide black shales (134.2 ppm; Ketris and Yudovich, 2009), the UCC (168.4 ppm; Taylor and McLennon, 1985), the NASC (165.4 ppm; Gromet et al., 1984), world coal (68.5 ppm; Ketris and Yudovich, 2009), Chinese coal (137.9 ppm; Dai et al., 2008) and USA coal (62.1 ppm; Finkelman, 1993)). According to Seredin and Dai's (2012) classification based on the outlook coefficient, the samples mainly have promising REY concentrations (mean C_{outl} = 1.33) in terms of economic viability (Fig. 18).

In the upper portion of well WA1331, REY content appears to roughly coincide with TOC (Fig. 17B); lower TOC zones also typically display lower REY concentrations and vice versa. This pattern is not, however, apparent in the other wells. Normalized to the UCC, the samples exhibit positive Eu anomalies and distinct negative Ce anomalies (Fig. 19). The samples display strong M-type ($La_N/Sm_N < 1$, $Gd_N/Lu_N > 1$) distribution as classified by Seredin and Dai (2012).

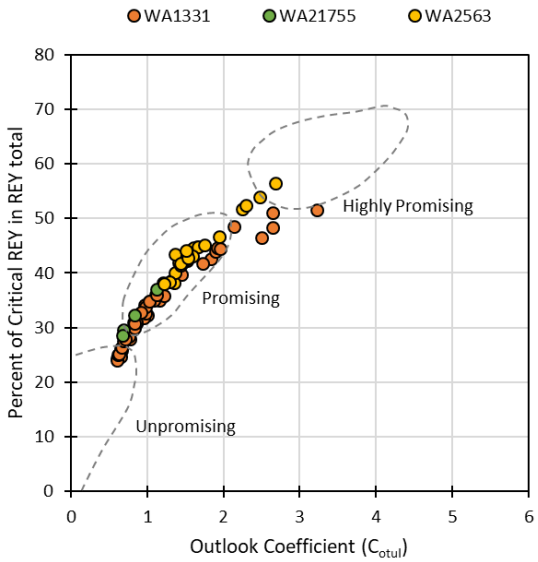

Figure 18. *(A) REY classification of the Besa River Formation samples (modified after Seredin and Dai, 2012). REY concentration and TOC vs. depth for wells (B) WA1331, upper portion, (C) WA1331, lower portion, and (D) WA2563.*

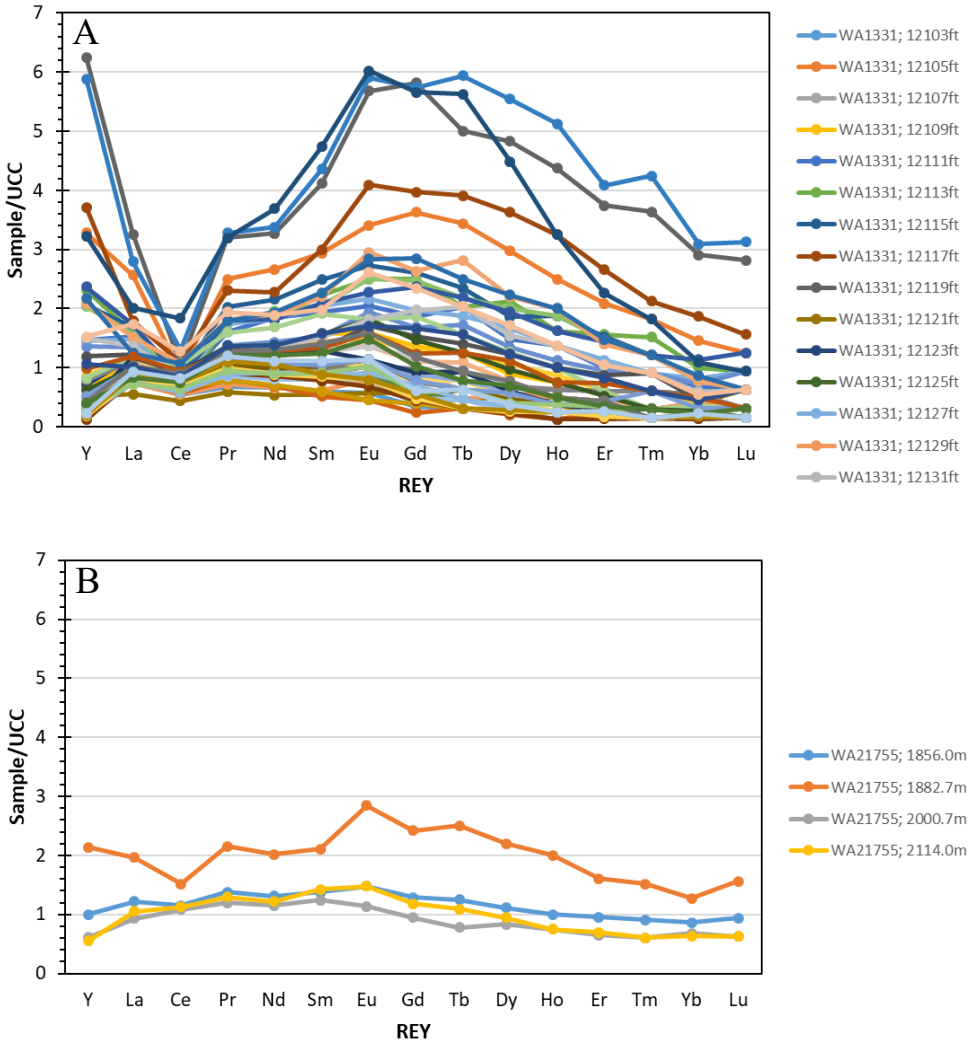

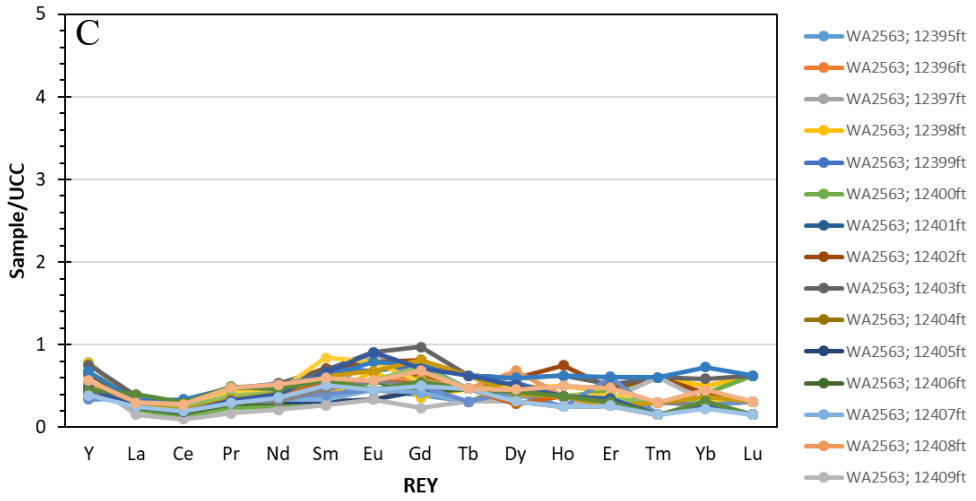

Figure 19. *UCC-normalized REE distribution patterns of the Besa River Formation samples from wells (A) WA1331, (B) WA21755, and (C) WA2563.*

3.6 Montney Formation

Samples from the Triassic Montney Formation are composed of shale and were retrieved from 12 wells. The average ∑REY concentration for all samples from all wells is 132.8 ppm (with an average ∑REY ranging from 106.8 ppm to 159.6 ppm for individual wells). The average ∑REY content (132.8 ppm) is comparable to worldwide black shales (134.2 ppm; Ketris and Yudovich, 2009) and Chinese coal (137.9 ppm; Dai et al., 2008); higher than world coal (68.5 ppm; Ketris and Yudovich, 2009) and USA coal (62.1 ppm; Finkelman, 1993); but lower than the UCC (168.4 ppm; Taylor and McLennon, 1985) and the NASC (165.4 ppm; Gromet et al., 1984).

According to the Seredin and Dai (2012) classification based on the outlook coefficient, samples from all the wells have promising REY concentrations (mean C_{outl} = 1.01, ranging from 0.88 to 1.14 between wells) (Fig. 20). Normalized to the UCC, the samples mainly exhibit weak positive Eu anomalies (but weak negative for two wells) and negative Ce anomalies (Fig. 21). The samples display M-type ($La_N/Sm_N < 1$, $Gd_N/Lu_N > 1$) to H-type ($La_N/Lu_N < 1$) distribution as classified by Seredin and Dai (2012).

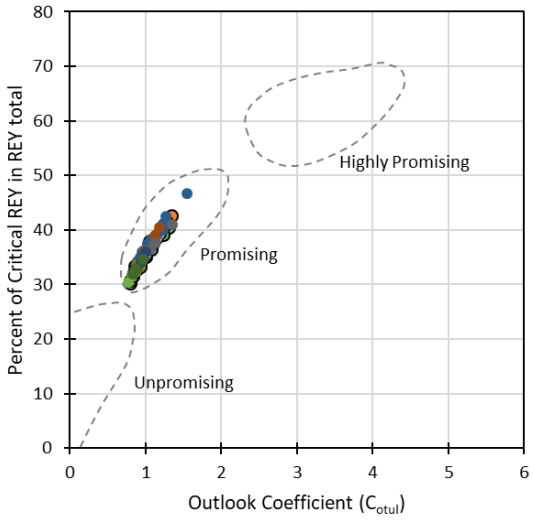

Figure 20. *(A) REY classification of the Montney Formation samples (modified after Seredin and Dai, 2012). REY concentration and TOC vs. depth for wells (B) 1-28-70-9W6, (C) B-35-G/93-P-01, and (D) 141258 CMS.*

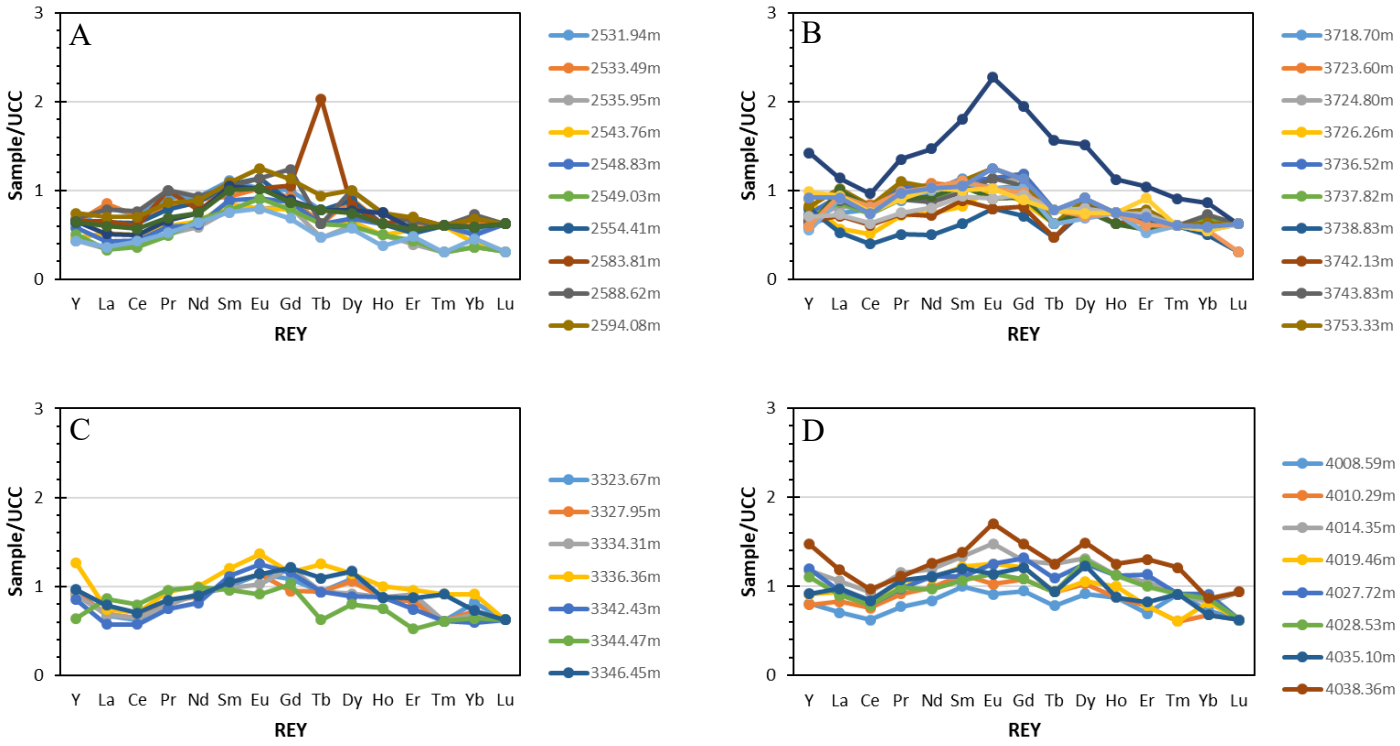

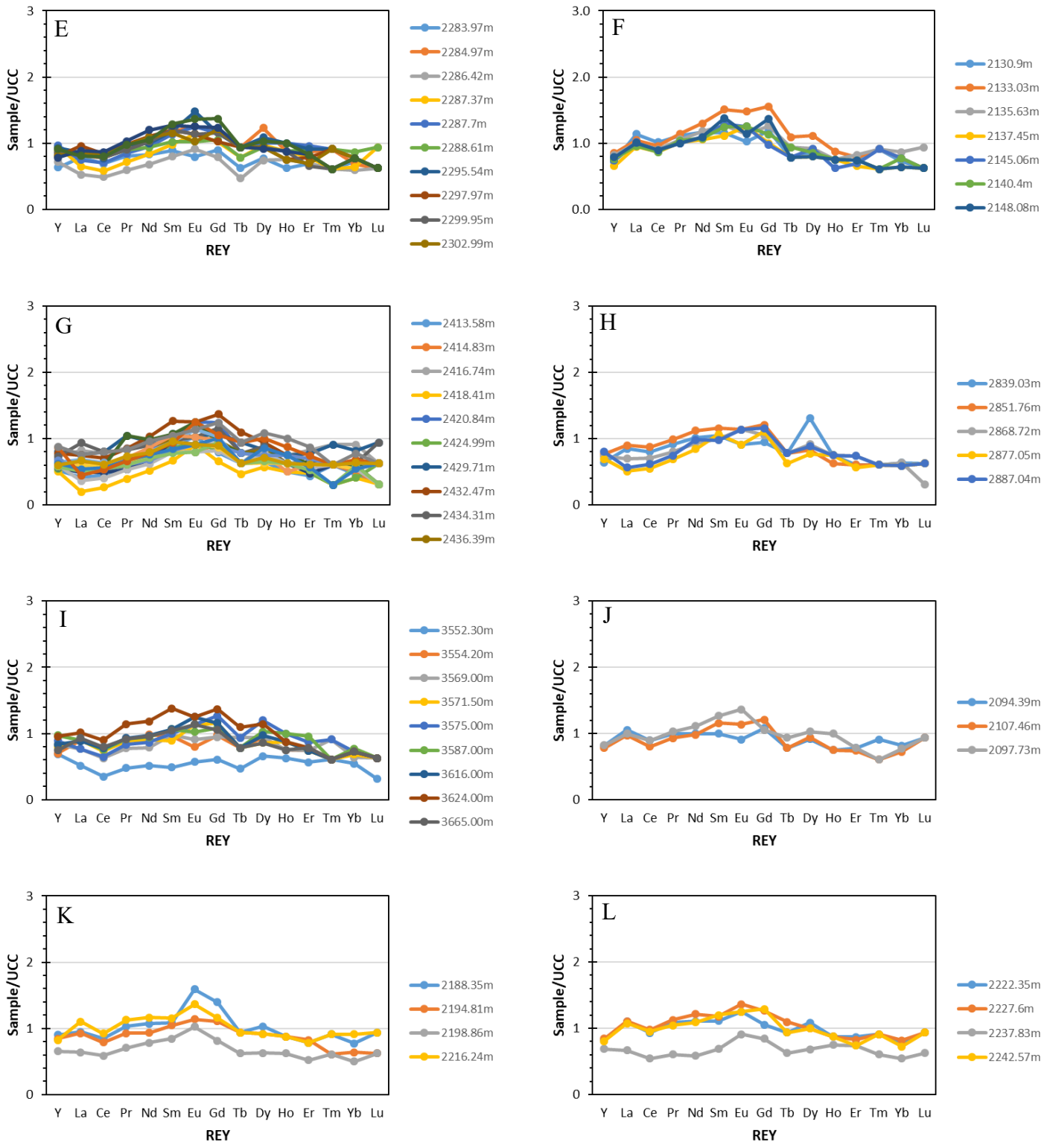

Figure 21. *UCC-normalized REE distribution patterns of the Montney Formation samples from wells (A)1-28-70-9W6, (B) B-35-G/93-P-01, (C) C-81-J/93-P-7, (D) B-52-I/93-P-6, (E) 14-13-78-16W6, (F) 4-19-77-10W6, (G) 141258 CMS, (H) 16-29-69-10W6, (I) SP1-10, (J) 07-34-078-11W6, (K)06-14-078-11W6, and (L) 15-30-077-10W6.*

3.7 Kanguk Formation

Samples from the late Cretaceous Kanguk Formation are comprised mainly of shale from Banks and Axel Heiberg islands, with some samples composed of bentonite from Banks Island in the Arctic. Average ∑REY concentrations are 182.1 ppm (range: 74.2–492.8 ppm) for the shales, and 221.3 ppm (range: 109.6–480.4 ppm) for the bentonites. These REY averages are higher than worldwide black shales (134.2 ppm; Ketris and Yudovich, 2009), the UCC (168.4 ppm; Taylor and McLennon, 1985), the NASC (165.4 ppm; Gromet et al., 1984), world coal (68.5 ppm; Ketris and Yudovich, 2009), Chinese coal (137.9 ppm; Dai et al., 2008) and USA coal (62.1 ppm; Finkelman, 1993).

According to the Seredin and Dai (2012) classification based on the outlook coefficient, the samples mainly lie in the unpromising to promising range in terms of economic viability (Fig. 22). The shale samples present an average C_{outl} of 0.88, whereas the bentonites have a C_{outl} of 1.13; these averages are above the 0.77 cut-off proposed by Seredin and Dai (2012). Normalized to the UCC, the samples exhibit mainly weak negative Eu anomalies and weak negative Ce anomalies (Fig. 23). Ce anomalies could not be determined for the bentonites as La data was not gathered, which is utilized in the Ce anomaly calculation. The samples display M-type ($La_N/Sm_N < 1$, $Gd_N/Lu_N > 1$) distribution, with samples from Sachs River ranging from M-type to H-type distribution as classified by Seredin and Dai (2012).

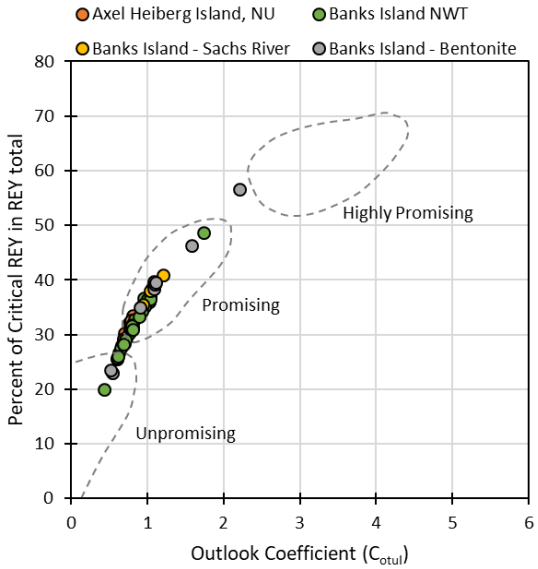

Figure 22. *REY classification of the Kanguk Formation samples (modified after Seredin and Dai, 2012).*

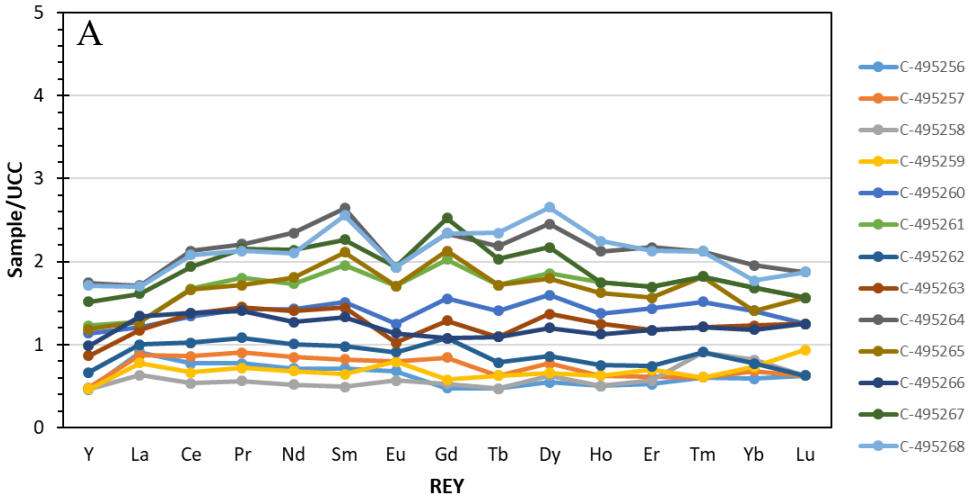
A
Sample/UCC
0
1
2
3
4
5
Y
La
Ce
Pr
Nd
Sm
Eu
Gd
Tb
Dy
Ho
Er
Tm
Yb
Lu
REY
C-495256
C-495257
C-495258
C-495259
C-495260
C-495261
C-495262
C-495263
C-495264
C-495265
C-495266
C-495267
C-495268

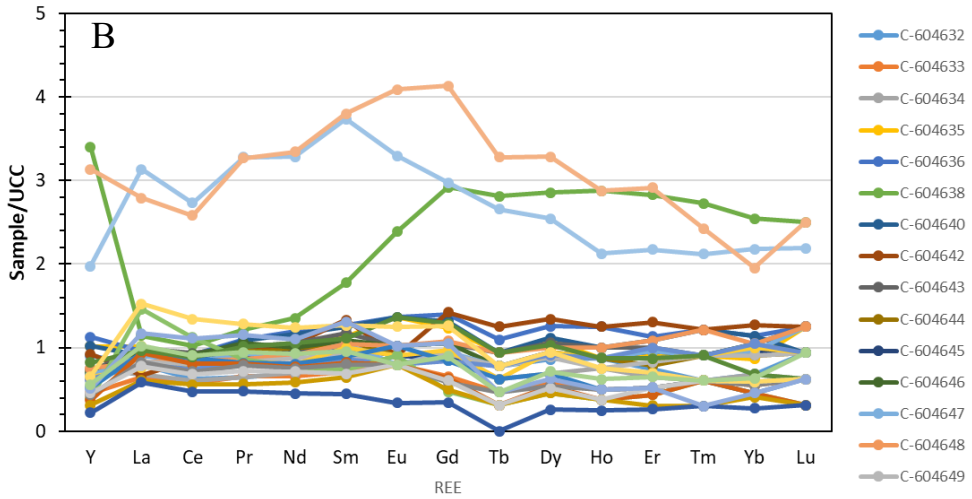
B
Sample/UCC
0
1
2
3
4
5
Y
La
Ce
Pr
Nd
Sm
Eu
Gd
Tb
Dy
Ho
Er
Tm
Yb
Lu
REE
C-604632
C-604633
C-604634
C-604635
C-604636
C-604638
C-604640
C-604642
C-604643
C-604644
C-604645
C-604646
C-604647
C-604648
C-604649

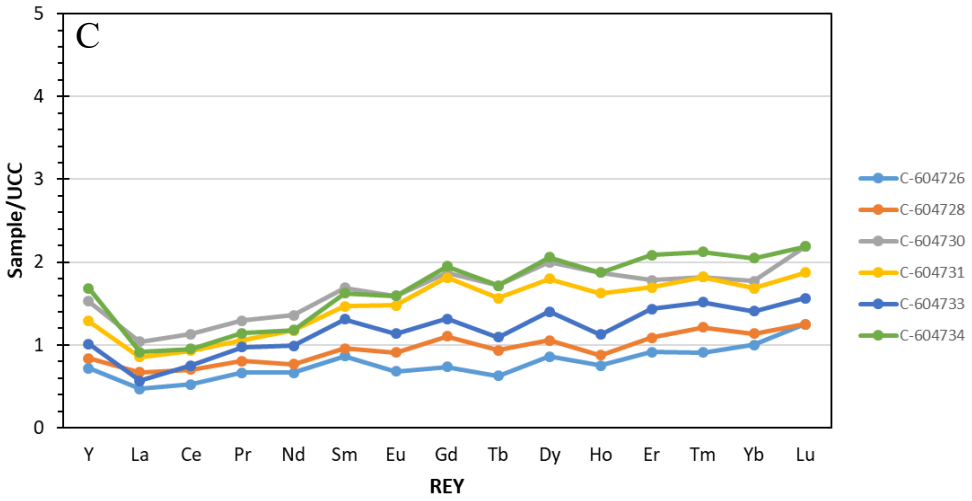
C
Sample/UCC
0
1
2
3
4
5
Y
La
Ce
Pr
Nd
Sm
Eu
Gd
Tb
Dy
Ho
Er
Tm
Yb
Lu
REY
C-604726
C-604728
C-604730
C-604731
C-604733
C-604734

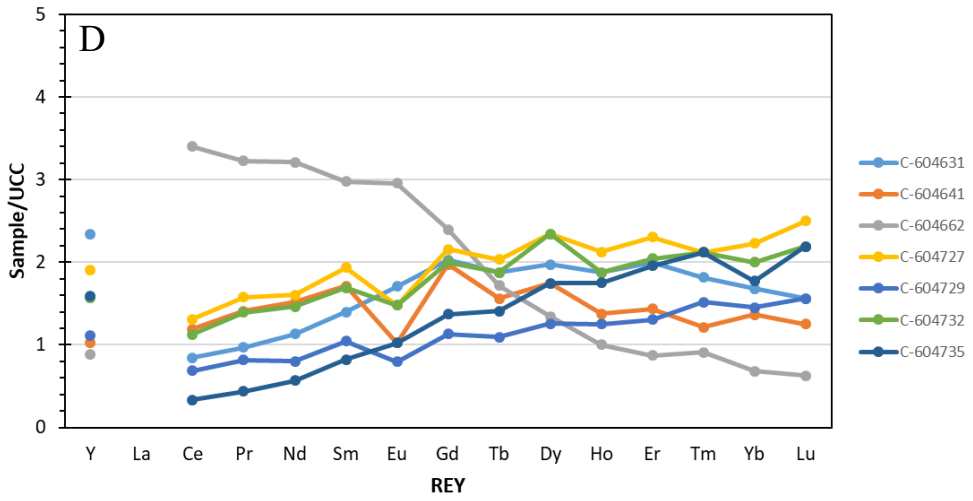

Figure 23. *UCC-normalized REE distribution patterns of the Kanguk Formation samples from (A) Banks Island, (B) Sachs River on Banks Island, (C) bentonite on Banks Island, and (D) Axel Heiberg Island.*

3.8 Second White Specks Formation and Belle Fourche Formation

Samples from the middle Cretaceous Second White Specks Formation and the Belle Fourche Formation are composed of shale and were retrieved from a well (7-29-42-12) in Alberta. Average ∑REY concentrations are 136.8 ppm (range: ppm) for samples of the Second White Specks Formation, and 137.6 ppm for samples of the Belle Fourche Formation. These values are comparable to average ∑REY concentrations of worldwide black shales (134.2 ppm; Ketris and Yudovich, 2009) and Chinese coal (137.9 ppm; Dai et al., 2008), but lower than the UCC (168.4 ppm; Taylor and McLennon, 1985) and the NASC (165.4 ppm; Gromet et al., 1984), and higher than world coal (68.5 ppm; Ketris and Yudovich, 2009) and USA coal (62.1 ppm; Finkelman, 1993).

According to the Seredin and Dai (2012) classification based on the outlook coefficient, samples from both the Second White Specks Formation and the Belle Forche Formation have promising REY concentrations (mean C_{outl} = 0.92 for both formations), in terms of economic viability (Fig. 24). Normalized to the UCC, samples from both formations exhibit weak positive Eu anomalies and negative Ce anomalies (Fig. 25). Samples from the Second White Specks Formation display M-type ($La_N/Sm_N < 1$, $Gd_N/Lu_N > 1$) distribution and the Belle Fourche samples display M-type to H-type ($La_N/Lu_N < 1$) distribution, as classified by Seredin and Dai (2012).

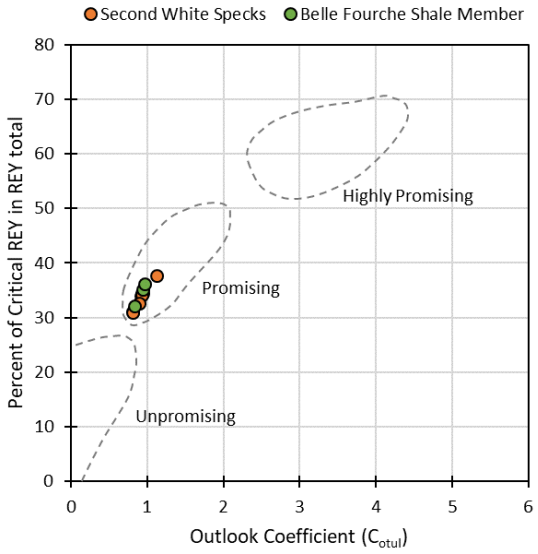

Figure 24. *REY classification of the Second White Specks Formation (2WS) and Belle Fourche samples from well 7-29-42-12 (modified after Seredin and Dai, 2012).*

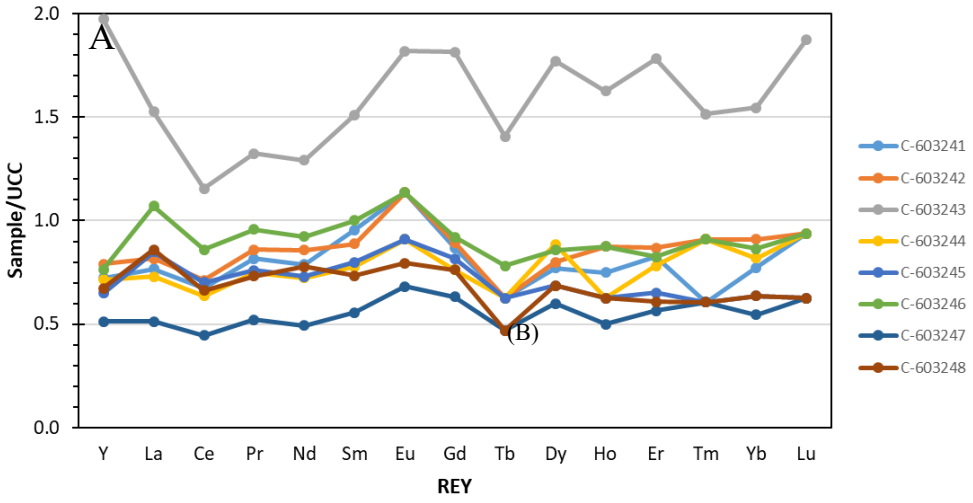

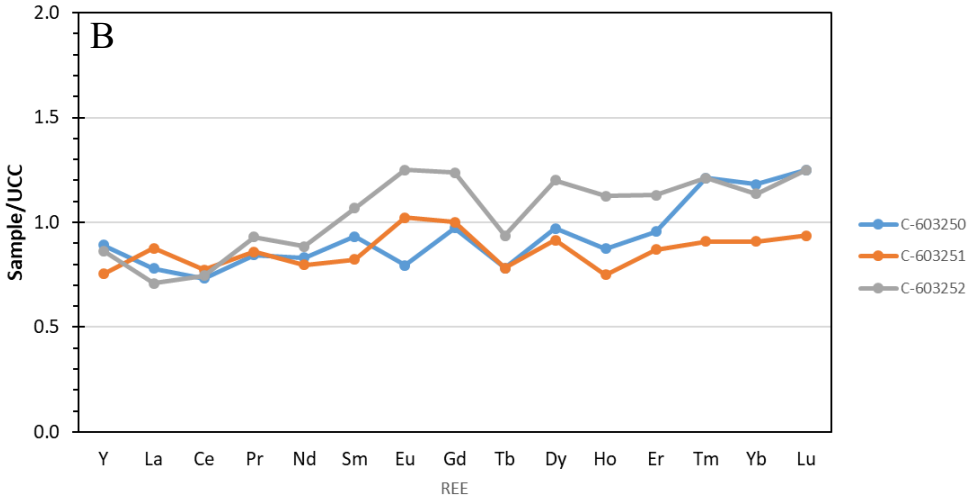

Figure 25. *UCC-normalized REE distribution patterns of samples from well 7-29-42-12, where (A) are samples from the Second White Specks (2WS) Formation, and (B) are samples from the Belle Fourche Formation.*

4. Summary

The majority of studies on coal and coal combustion by-products REE estimation studies has been done on Chinese and United States resources. However, despite considerable amount of Canada recoverable coal reserves (6.6 billion tonnes) the few current studies are local and no systematic nationwide research has been done on the equivalent Canadian resource potential. One of the major purposes of this study was to organize the large collection of Canadian coal and coal combustion byproducts at the Geological Survey of Canada to evaluate the REE resource potential. Due to COVID limitations the analysis of Geological Survey of Canada coal collection in Calgary was not possible and we did a comprehensive literature review to identify the major knowledge gaps on REE resources and Canadian coal geochemistry. It is anticipated with return to normal post-pandemic situations we will be able to achieve this important goal in the next phases of TGI program.

However, initial studies on large geochemical datasets collected through Geo-Mapping for Energy and Minerals (GEM) and Geoscience for New Energy Supply (GNES) programs indicates that organic-rich shales in Canada show potential for REY resources (refer to Table 7 for REY data); such deposits include the Gordondale Member, Duvernay Formation, Formation, Utica Formation, Garbutt Formation, Besa River Formation, Montney Formation, Kanguk Formation, and the Second White Specks Formation.

The average REY concentrations of Canadian coal samples (Table 6) are roughly comparable to those of the Jungar and Daqingshan Coalfields in northern China (154–257 ppm), which are considered by Dai et al. (2012b) to be REE-enriched. They are however, lower in concentration than Chinese and USA coals (Table 3). The highly REY-enriched Chinese and USA coals are generally associated with the leaching of volcanic tonsteins.

The REY concentrations are comparable to Chinese and USA shales (Table 5). The REY contents do not appear to be specifically enriched in certain age units, nor are certain age units that are more economically viable in terms of critical elements. The average outlook coefficients of each Canadian formation are $0.7 \leq C_{outl} \leq 1.9$, which is promising in terms of economic viability, based on the Seredin and Dai (2012) classification. Normalized to the UCC (upper continental crust), the Canadian deposits mainly display MREE enrichment (M-type distribution), with some HREE enrichment. Weak positive Eu anomalies and negative Ce anomalies are predominant.

Table 7. *REY data for select Canadian deposits, displaying averages of the various wells in each formation. Refer to Table 5 for data on individual wells. Note that the Eu and Ce anomalies as well as the REY distribution type are based on UCC-normalized data.*

Formation	Age	Mean ∑REY (ppm)	Mean C_{outl}	Eu Anomaly	Ce Anomaly	REY Distribution Type
Gordondale	Lower Jurassic	179 – 213	1.72 - 1.96	Weak positive	Distinct negative	M to H
Duvernay	Devonian	130 – 149	1.06 - 1.15	Weak positive	Negative	M
Utica	Upper Ordovician	105 – 112	0.77 - 0.88	Weak positive, weak negative	Weak negative	L to M
Garbutt	Lower Cretaceous	71 – 234	0.83 - 1.21	Weak positive, weak negative	Weak negative	M to H
Besa River	Devonian	56 – 213	0.83 - 1.64	Positive	Distinct negative	M
Montney	Triassic	107 – 162	0.88 - 1.14	Weak positive	Negative	M to H
Kanguk	Upper Cretaceous	163 – 221	0.73 - 1.13	Weak negative, weak positive	Weak negative, weak positive	M to H
2WS	Middle Cretaceous	137	0.92	Weak positive	Negative	M
Belle Fourche	Middle Cretaceous	138	0.92	Weak positive	Negative	M to H

Acknowledgements

We would like to thanks Natural Resources Canada Targeted Geoscience Initiative (TGI) program manger for funding this study. All geochemical bulk REE data for this study was part of GNES shale reservoir characterisation. The initial version of this report significantly benefited from constructive comments of Dr. E. Potter, his inputs are really appreciated.

References

Balaram V., 2019. Rare earth elements: A review of applications, occurrence, exploration, analysis, recycling, and environmental impact. *Geoscience Frontiers* 10, 1285-1303. https://doi.org/10.1016/j.gsf.2018.12.005

Baron R., 2020. Determination of rare earth elements content in hard coal type 31.1. *Management Systems in Production Engineering* 28, 240-246.

Bai J.R., Wang Q., Wei Y.Z., Liu T., 2011. Geochemical occurrences of rare earth elements in oil shale from Huadian. *Journal of Fuel Chemistry and Technology* 39, 489-494.

Bau M., Schmidt K., Koschinsky A., Hein J., Kuhn T., Usui A., 2014. Discriminating between different genetic types of marine ferro-manganese crusts and nodules based on rare earth elements and yttrium. *Chemical Geology* 381, 1–9.

Binnemans, K., Jones, P.T., Blanpain, B., Van Gerven, T., Yang, Y., Walton, A. and Buchert, M., 2013. Recycling of rare earths: a critical review. *Journal of Cleaner Production* 51, 1-22.

Birdwell J.E., 2012. Review of Rare Earth Element Concentrations in Oil Shales of the Eocene Green River Formation. U.S. Geological Survey Open-File Report 2012–1016, 20 p.

Birk, D., White, J. C., 1991. Rare earth elements in bituminous coals and underclays of the Sydney Basin, Nova Scotia: Element sites, distribution, mineralogy. *International Journal of Coal Geology* 19, 219–251.

Berna Y.P., 2019. The REE Characteristics of Oil Shales in the Lower Eocene Celtek Formation (Yozgat, Turkey) and their Relation to Tectonic Provenance. *Acta Geologica Sinica* (English Edition) 93, 604–621.

Boynton W.V., 1985. Cosmochemistry of the rare earth elements: Meteorite studies. In: Henderson P. (ed.). Rare Earth Element Geochemistry. (Developments in Geochemistry). Amsterdam, Elsevier. 115-1522.

Caetano-Filho S., Paula-Santos G.M., Dias-Brito D., 2018. Carbonate REE+Y signatures from the restricted early marine phase of South Atlantic Ocean (late Aptian – Albian): The influence of early anoxic diagenesis on shale-normalized REE+Y patterns of ancient carbonate rocks. *Palaeogeography Palaeoclimatology Palaeoecology* 500, 69-83.

Cameron R., 2017. REE recovery from secondary sources. Available from: http://reechromite.ca/en/rare-earth-elements/research-and-development/all-reports/

Cimen O., Koc S., Sari A., 2013. Rare earth element (REE) geochemistry and genesis of oil shales around Dağhacilar Village, Göynük-bolu, Turkey. *Oil Shale* 30, 419-440.

Condie K.C., 1991. Another look at rare elements in shales. *Geochimica et Cosmochimica Acta* 55, 2521-2531.

Costis S., Mueller K.K., Blais J.F., 2019. Review of recent work on the recovery of rare earth elements from secondary sources: Final report No. R1859. Available from: http://espace.inrs.ca/id/eprint/9445/1/R1859.pdf

Crowley S.S., Stanton R.W., Ryer T.A., 1989. The effects of volcanic ash on the maceral and chemical composition of the C coal bed, Emery Coalfield, Utah. *Organic Geochemistry* 14, 315–331.

Dai S., Li D., Chou C.L., Zhao L., Zhang Y., Ren D., Ma Y., Sun Y., 2008. Mineralogy and geochemistry of boehmite-rich coals: new insights from the Haerwusu Surface Mine, Jungar Coalfield, Inner Mongolia, China. *International Journal of Coal Geology* 74, 185–202.

Dai S., Jiang Y., Ward C.R., Gu L., Seredin V.V., Liu H., Zhou D., Wang X., Sun Y., Zou J., Ren D., 2012a. Mineralogical and geochemical compositions of the coal in the Guanbanwusu Mine, Inner Mongolia, China: further evidence for the existence of an Al (Ga and REE) ore deposit in the Jungar Coalfield. *International Journal of Coal Geology* 98, 10–40.

Dai S., Ren D., Chou C.L., Finkelman R.B., Seredin V.V., Zhou Y., 2012b. Geochemistry of trace elements in Chinese coals: A review of abundances, genetic types, impacts on human health, and industrial utilization. *International Journal of Coal Geology* 94, 3-21.

Dai S., Graham I.T., Ward C.R., 2016a. A review of anomalous rare earth elements and yttrium in coal. *International Journal of Coal Geology* 159, 82-95.

Dai S., Liu J., Ward C.R., Hower J.C., French D., Jia S., Hood M.M., Garrison T.M., 2016b. Mineralogical and geochemical compositions of Late Permian coals and host rocks from the Guxu Coalfield, Sichuan Province, China, with emphasis on enrichment of rare metals. *International Journal of Coal Geology* 166, 71-95.

Dai S., Yan X., Ward C.R., Hower J.C., Zhao L., Wang X., Zhao L., Ren D., Finkelman R.B., 2016c. Valuable elements in Chinese coals: A review. *International Geology Review* 60, 590-620.

Dai S, Xie P, Jia S, Ward CR, Hower HC, Yan X, French D., 2017. Enrichment of U-Re-V-Cr-Se and rare earth elements in the Late Permian coals of the Moxinpo Coalfield, Chongqing, China: genetic implications from geochemical and mineralogical data. *Ore Geology Review* 80, 1–17.

Dai S., Finkelman, R.B., 2017. Coal as a promising source of critical elements: Progress and future prospects. *International Journal of Coal Geology* 186, 155-164.

Dostal J., 2017. Rare earth element deposits of alkaline igneous rocks. Resources 6, 34, 2017.

Emsbo P., McLaughlin P.I., Breit G.N., du Bray, E.A., Koenig A.E., 2015. Rare earth elements in sedimentary phosphate deposits: Solution to the global REE crisis? *Gondwana Research* 27, 776–785.

Dutta, T., Kim, K.H., Uchimiya, M., Kwon, E.E., Jeon, B.H., Deep, A. and Yun, S.T., 2016. Global demand for rare earth resources and strategies for green mining. *Environmental research* 150, 182-190.

Fakhry A.A, Eid K.A., Mahdy A.A., 1998. Distribution of REE in shales overlying the Abu Tartur phosphorite deposit, Western Desert, Egypt. *Journal of alloys and compounds* 275, 929–933.

Finkelman R.B., 1993. Trace and minor elements in coal. In: Engel MH, Macko SA, (eds.) Organic Geochemistry. Plenum, New York. p. 593–607.

Finkelman R.B., Dai S, French D., 2019. The importance of minerals in coal as the hosts of chemical elements: A review. *International Journal of Coal Geology* 212, 103251.

Flier-Keller, E. van der., 1993. Earth Elements in Western Canadian Coals. *Energy Sources* 15, 623–638.

Folgueras, M.B., Alonso, M. and Fernández, F.J., 2017. Coal and sewage sludge ashes as sources of rare earth elements. *Fuel* 192, 128-139.

Freslon N., Bayon G., Toucanne S., Bermall S., Bollinger C., Cheron S., Etoubleau J., Germain Y., Khripounoff A., Ponzevera E., Rouget, M.L., 2014. Rare earth elements and neodymium isotopes in sedimentary organic matter. *Geochimica et Cosmochimica Acta* 140, 177–198.

Fu X., Wang J., Zeng Y., Tan F., Feng X., 2010. REE geochemistry of marine oil shale from the Changshe Mountain area, northern Tibet, China. *International Journal of Coal Geology* 81, 191–199.

Fu X., Wang J., Zeng Y., Tan F., He J., 2011. Geochemistry and origin of rare earth elements (REEs) in the Shengli River oil shale, northern Tibet, China. *Geochemistry* 71, 21-30.

Goodarzi F., Grieve D.A., Labonte M., 1990. Mineralogical and elemental composition of tonsteins from the East Kootenay Coalfields, Southeastern British Columbia. *Energy Sources* 12, 265-295.

Goodarzi, F., 2002. Mineralogy, elemental composition and modes of occurrence of elements in Canadian feed-coals. *Fuel* 81, 1199-1213.

Goodarzi F., Gentzis T., 2018. Elemental concentration and organic petrology of unique liptinite-rich humic coal, canneloid shale, and cannel coal of Devonian age from Arctic Canada. *Chemical Geology* 485, 44-55.

Goodenough, K.M., Wall, F., Merriman, D., 2018. The Rare Earth Elements: demand, global resources, and challenges for resourcing future generations. *Natural Resources Research* 27, 201-216.

Gromet L.P., Dymek R.F., Haskin L.A., Korotev R.L., 1984. The ″North American shale composite”: its compilation, major and trace element characteristics. *Geochimica et Cosmochimica Acta* 48, 2469–2482.

Hower J.C., Groppo J.G., Henke K.R., Hood M.M., Eble C.F., Honaker R.Q., Zhang W., Qian D., 2015. Notes on the potential for the concentration of rare earth elements and Yttrium in coal combustion fly ash. *Minerals* 5, 356-366.

Hower J.C., Eble C.F., Dai S., Belkin H.E., 2016. Distribution of rare earth elements in eastern Kentucky coals: Indicators of multiple modes of enrichment? *International Journal of Coal Geology* 160-161, 73-81.

Hower J., Eble C., Backus J., Xie P., Liu J., Fu B., Hood M., 2020a. Aspects of rare earth element enrichment in Central Appalachian coals. *Applied Geochemistry* 120, 104676

Hower J.C., Qian D., Briot N.J., Hood M.M., Eble C.F., 2020b. Mineralogy of a rare earth element-rich Manchester coal lithotype, Clay County, Kentucky. *International Journal of Coal Geology* 220,103413.

Hussain R., Luo K., 2020. Geochemical Evaluation of Enrichment of Rare-Earth and Critical Elements in Coal Wastes from Jurassic and Permo-Carboniferous Coals in Ordos Basin, China. *Natural Resources Research* 29, 1731-1754.

Jin L., Ma L., Dere A., White T., Mathur R., Brantley S.L., 2017. REE mobility and fractionation during shale weathering along a climate gradient. *Chemical Geology* 466, 352-379.

Ketris M.P., Yudovich Y.E., 2009. Estimations of Clarkes for Carbonaceous biolithes: world averages for trace element contents in black shales and coals. *International Journal of Coal Geology* 78,135.

Kuppusamy, V. K., Holuszko, M., 2019a. Rare earth elements in flotation products of coals from East Kootenay coalfields, British Columbia. *Journal of Rare Earths*, 37, 1366–1372.

Kuppusamy, V.K., Holuszko, M.E., 2019b. Characterization and extraction of rare-earth elements from East Kootenay coalfield samples, southeastern British Columbia; *in* Geoscience BC Summary of Activities 2018: Minerals and Mining, Geoscience BC, Report 2019-1, p. 33–44.

Kuppusamy, V.K. Holuszko, M.E., 2020. Development of a database of rare-earth element occurrences and characteristics for the East Kootenay coalfields of southeastern British Columbia (NTS 082G/10, 15): proposed work; *in* Geoscience BC Summary of Activities 2019: Minerals, Geoscience BC, Report 2020-01, p. 51–54.

Kuppusamy, V.K. Holuszko, M.E., 2021, Development of rare-earth elements database for the East Kootenay coalfield of southeastern British Columbia (NTS 082G/10, 15) using field collected samples: preliminary results; *in* Geoscience BC Summary of Activities 2020: Minerals, Geoscience BC, Report 2021-01, p. 67–74.

Kuppusamy, V. K., Holuszko, M., 2022. Sulfuric acid baking and water leaching of rare earth elements from coal tailings. *Fuel*, 319, 123738.

Lefticariu L., Klitzing K.L., Kolker, A., 2020. Rare Earth Elements and Yttrium (REY) in coal mine drainage from the Illinois Basin, USA. *International Journal of Coal Geology* 217, 1-16.

Lev S.M., Filer J.K., 2004. Assessing the impact of black shale processes on REE and the U–Pb isotope system in the southern Appalachian Basin. *Chemical Geology* 206, 393– 406.

Li Z., Li X., Zhang L., Li S., Chen J., Feng X., Zhao D., Wang Q., Gao Z., Xiong B., 2020. Partitioning of rare earth elements and yttrium (REY) in five coal-fired power plants in Guizhou, Southwest China. *Journal of Rare Earths* 38, 1257-1264.

Ma L., Jin L., Brantley S.L., 2011. How mineralogy and slope aspect affect REE release and fractionation during shale weathering in the Susquehanna/Shale Hills Critical Zone Observatory. *Chemical Geology* 290, 31-49.

Mastalerz M., Drobniak A., Eble C., Ames P., McLaughlin P., 2020. Rare earth elements and yttrium in Pennsylvanian coals and shales in the eastern part of the Illinois Basin. *International Journal of Coal Geology* 231, 103620.

McLennan S.M., 1989. Rare earth elements in sedimentary rocks: influence of provenance and sedimentary processes. *Review in Mineralogy* 21, 169–200.

Middleton A., Park D.M., Jiao Y., Hsu-Kim, H., 2020. Major element composition controls rare earth element solubility during leaching of coal fly ash and coal by-products. *International Journal of Coal Geology* 227,103532.

Mishra V., Chakravarty S., Finkelman R.B., Varma A.K., 2019. Geochemistry of Rare Earth Elements in Lower Gondwana Coals of the Talchir Coal Basin, India. *Journal of Geochemical Exploration* 204, 43-56.

Mutlu B.K., Cantoni B., Turolla A., Antonelli M., Hsu-Kim H., Wiesner M.R., 2018. Application of nanofiltration for Rare Earth Elements recovery from coal fly ash leachate: Performance and cost evaluation. *Chemical Engineering Journal* 349, 309-317.

Natural Resources Canada (NRCan) REE Facts, 2022. https://www.nrcan.gc.ca/our-natural-resources/minerals-mining/minerals-metals-facts/rare-earth-elements-facts/20522

Noack C.W., Jain J.C., Stegmeier J., Hakala J.A., Karamalidis A.K., 2015. Rare earth element geochemistry of outcrop and core samples from the Marcellus Shale. *Geochemical Transactions* 16, 1-11.

Park S., Kim M., Lim Y., Yu J., Chen S., Woo S.W., Yoon S., Bae S., Kim H.S., 2020. Characterization of rare earth elements present in coal ash by sequential extraction. *Journal of Hazardous Materials* 402, 123760.

Phan T.T., Hakala J.A., Lopano C.L., Sharma S., 2019. Rare earth elements and radiogenic strontium isotopes in carbonate minerals reveal diagenetic influence in shales and limestones in the Appalachian Basin. *Chemical Geology* 509, 194–212.

Piper D.Z., 1974. Rare earth elements in the sedimentary cycle: A summary. *Chemical Geology* 14, 285–304.
Rosita W., Bendiyasa I.M., Perdana I., Anggara F., 2020. Sequential particle-size and magnetic separation for enrichment of rare earth elements and yttrium in Indonesia coal fly ash. *Journal of Environmental Chemical Engineering* 8, 103575.
Roth, E., Alvin, M. A., 2020. Locating and extracting Rare Earth Elements from domestic coal-based resources. *Advanced Materials & Processes*, 178, 24–27.
Sarswat P.K., Leake M., Allen L., Free M.L., Hu X., Kim D., Noble A., Luttrell G.H., 2020. Efficient recovery of rare earth elements from coal based resources: a bioleaching approach. *Materials Today Chemistry* 16, 100246.
Seredin, V.V., 2010. A new method for primary evaluation of the outlook for rare earth element ores. *Geology of Ore Deposits* 52, 428–433.
Seredin V.V., Dai S., 2012. Coal deposits as potential alternative sources for lanthanides and yttrium. *International Journal of Coal Geology* 94, 67-93.
Simandl, G.J., 2014. Geology and market-dependent significance of rare earth element resources. *Mineralium Deposita*, 49, 889-904.
Sholkovitz, E.R. and Elderfield, H., 1988. Cycling of dissolved rare earth elements in Chesapeake Bay. *Global Biogeochemical Cycles*, 2, 157-176.
Taylor S.R. McLennan S.M., 1985. The continental crust: Its composition and evolution. Blackwell, Oxford. 312 pp.
Turner E.C., 2015. Base-metal Enrichment in Stage-5 (mid-Cambrian) Black Shale of the Hess River Formation, Misty Creek Embayment, Selwyn Basin. In: Paradis S., (Ed.). Targeted Geoscience Initiative 4: sediment-hosted Zn-Pb deposits: processes and implications for exploration; Geological Survey of Canada, Open File 7838, 297 p.
U.S. Department of Energy, 2011. 2011 Critical Materials Strategy. https://energy.gov/sites/prod/files/DOE_CMS2011_FINAL_Full.pdf
U.S. Geological Survey, 2017. Mineral commodity summaries. U.S. Department of interior. 202 p., https://doi.org/10.3133/70180197.
U.S. Geological Survey, 2022. Mineral commodity summaries. U.S. Department of interior. 202 p., https://doi.org/10.3133/mcs2022.
Wang Q., Bai J., Ge J., Wei Y.Z., Li S., 2014. Geochemistry of rare earth and other trace elements in Chinese oil shale. *Oil Shale* 31, 266-277.
Yang J., Torres M., McManus J., Algeo T.J., Hakala J.A., Verba C., 2017. Controls on rare earth element distributions in ancient organic-rich sedimentary sequences: Role of post-depositional diagenesis of phosphorus phases. *Chemical Geology* 466, 533-544.
Yang J., Verba C., Torres M., Hakala J.A., 2018. Empirically assessing the potential release of rare earth elements from black shale under simulated hydraulic fracturing conditions. *Journal of Natural Gas Science and Engineering* 50, 259-268.
Zanin Y.N., Eder V.G., Zamirailova A.G., Krasavchikov V.O., 2010. Models of the REE distribution in the black shale Bazhenov Formation of the West Siberian marine basin, Russia. *Geochemistry* 70, 363-376.
Zhang W., Honaker R., 2019. Enhanced leachability of rare earth elements from calcined products of bituminous coals. Minerals Engineering 142, 105935.
Zinck, J., 2013. Realizing Canada's Rare Earth Elements resource potential: R&D perspectives. In: London, I.M., Goode, J.R., Moldoveanu, G., Rayat M.S. (eds.) Proceedings of the 52nd Conference of Metallurgists (Com), October 27 to 31, 2013, Montréal, Québec, Canada. 25-35.